Applied Mathematical Modelling 41 (2017) 375–398

Contents lists available at ScienceDirect

Applied Mathematical Modelling

journal homepage: www.elsevier.com/locate/apm

Optimising prediction model of centrifugal pump as turbine with viscosity effects

Wen-Guang Li

Department of Fluid Machinery, Lanzhou University of Technology, 730050 Lanzhou, Gansu, China

ARTICLE INFO

Article history:
Received 6 October 2015
Revised 9 July 2016
Accepted 5 September 2016
Available online 12 September 2016

Keywords:
Centrifugal pump
Pump as turbine
Viscosity
Reynolds number
Conversion factor
CFD

ABSTRACT

Performance conversion of a centrifugal pump as turbine from the known performance curves in pump mode is vital important in pump selection, power generation and investment assessment, especially under low Reynolds number operation conditions. Effects of Reynolds number on such a performance conversion have not been taken into account so far. In the paper, flow rate, head and output power and hydraulic efficiency conversion factors at zero efficiency/power, 0.8 part-load, best efficiency, 1.2 over-load and maximum flow rate points are defined and extracted from the performance curves of a centrifugal pump as turbine at five viscosities obtained by using CFD simulations. The conversion factors are correlated to impeller Reynolds number and a performance conversion model is proposed by employing 3rd and 4th order polynomials for the output power and head curves. New correlations of flow rate, head and efficiency conversion factors are also attempted in terms of specific speed and efficiency as well as impeller Reynolds number based on the data found in literature. The conversion model is a framework and can be useful for design of pump as turbine and its performance prediction, especially under variable liquid viscosity conditions.

1. Introduction

A centrifugal pump can work in the reverse direction as a renewable energy generator in micro-hydro-power plants [1–7] or as a power recovery turbine in the process industry, such as reverse osmosis, hydrocarbon process, gas scrubbing process, ammonia production, petroleum cracking process, hot water circulation system and so on [8–10]. Compared with normal hydro-turbines, a pump as turbine (PAT) is cheaper and more viable and available for choice. Thus PATs can play an important role in reduction of carbon dioxide emission and maintenance of sustainable development of human being.

In order to select a suitable centrifugal pump for a specific turbine application, it is needed to know how to predict the turbine performance based on a pump performance available. In consequence, various methods have been proposed to estimate the performance in turbine mode [10–17]. In these methods, the flow rate, head and efficiency in the turbine model are correlated to counterparts in the pump mode by means of conversion factors at the best efficiency points (BEP) in both modes. If the performance parameters and conversion factors at BEP are known in the pump mode, then the performance parameters at BEP in the turbine mode can be figured out. Various conversion factors are summarised in Appendix A.

In particular, the torque and head curves of PAT are assumed to be a parabolic function of flow rate, and five coefficients in those parabolic curves are determined by the torque, head, and their derivatives with respect to flow rate at BEP; finally, one can use those coefficients to predict PAT torque and head curve, and subsequently the efficiency curve in [11]. The head and output power curves of PAT are predicted by making use of Hermit spline interpolation method in [16] according to the

E-mail address: Liwg40@sina.com

http://dx.doi.org/10.1016/j.apm.2016.09.002
0307-904X/

Nomenclature

a	coefficient in 3rd or 4th order polynomials
d_{1t}	impeller inlet diameter in turbine mode, m
d_{2p}	impeller outlet diameter in pump mode, $d_{1t} = d_{2p}$, m
g	acceleration due to gravity, m/s^2
h	head conversion factor
h_e	impeller theoretical head conversion factor
H	head, m
H_L	hydraulic loss, m
K_p	international dimensionless specific speed in pump mode, $K_p = (\frac{\pi n_p}{30})\sqrt{Q_p}/(gH_p)^{3/4}$
n	impeller rotating speed in pump or turbine mode, r/min
N_p	specific speed in pump mode in Europe, $N_p = n_p\sqrt{Q_p}/H_p^{3/4}$, (r/min, m^3/s, m), $N_p = 52.9K_p$
n_{sp}	specific speed in pump mode in China and Russia, $n_{sp} = 3.65n_p\sqrt{Q_p}/H_p^{3/4}$, (r/min, m^3/s, m), $n_{sp} = 193.2K_p = 3.65N_p$
m	number of points on performance curves in turbine mode
P	output power, kW
q	flow rate conversion factor
Q	flow rate, m^3/s or l/s
r_{1t}	radius of impeller inlet in turbine mode, m, $r_{1t} = 0.5d_{1t}$
Re	impeller Reynolds number
u_{1t}	impeller tip speed in turbine mode, m/s

Greek symbols

β_2	exit blade angle, deg
δ	dimensionless root-mean-square error
ε	hydraulic efficiency conversion factor
η	efficiency
κ	hydraulic loss conversion factor
λ	output power conversion factor
ν	fluid kinematic viscosity, cSt(mm^2/s)
ρ	fluid density, kg/m^3

Superscripts

CFD	obtained from CFD simulations
mod	obtained from the model of conversion factors

Subscripts

0	at zero efficiency/output power point
0.8	flow rate at 0.8BEP or 0.8 part-load point
1	BEP
1.2	flow rate at 1.2BEP or 1.2 over-load point
ref	reference condition
H	head
m	mechanical efficiency
max	maximum flow rate
p	pump mode
P	output power
t	turbine mode
v	volumetric efficiency
w	water
η	hydraulic or total efficiency

performance parameters and their derivatives at zero power point (ZPP) or zero efficiency point (ZEP) and BEP. Further, the ratios of PAT head and output power at any operational point to the head and power at BEP are expressed by means of a parabolic function and 3rd order polynomial of the ratio of the flow rate at any operational point to the flow rate at BEP, respectively; the head and power can be estimated by using these expressions at any operational points in [18].

A series of experiments on performance and flow of PAT were carried out in [17–23], and our understanding about PAT performance and inside flow features have been improved in a great deal. Recently, CFD methods have been applied in PAT

performance prediction and flow pattern characterization. Steady turbulent flows in PAT were investigated by using various CFD codes and the performance curves of PAT were obtained in [24–28]. Unsteady flow fields in PAT were studied by means of moving mesh technique in CFD codes and its transient characteristics were clarified numerically in Morros et al. [29,30]. The steady and unsteady radial thrusts were identified by using CFD simulations in [24,26,31].

In these studies water is used only. This situation doesn't seem proper for PATs in the petroleum cracking process where the fluid is often more viscous than water. Thus effects of liquid viscosity on PAT performance and flow pattern were exploited in [32]. However, the method for performance curves conversion from water in the pump mode to those of a liquid with viscosity more than water in turbine mode is not proposed.

In this article, a method for establishing PAT performance curves is put forward based on the head, output power and hydraulic efficiency conversion factors at five operational points such as ZEP, 0.8BEP, BEP, 1.2BEP and maximum flow rate in turbine mode as well as the head, hydraulic efficiency at BEP in pump mode when both modes are in the same rotational speed at various viscosities of liquid. The conversion factors are correlated to impeller Reynolds number. In the method, 3rd and 4th order polynomials are employed to stand for the head and output power curves. Further, new correlations of flow rate, head and efficiency conversion factors at BEP are established in terms of specific speed as well as impeller Reynolds number based on the performance data of PAT found in literature.

Compared with the performance conversion methods existing in [11,16,18], the presently proposed approach possesses the following evident features: (1) it is simple because just 3rd and 4th order polynomials defined by four and five points are needed to describe the shaft/output power and head curves, respectively, (2) the first derivatives of the shaft/output power and head with respect to the flow rate are not required, and no additional errors are induced; (3) the effect of viscosity or impeller Reynolds number is taken into account.

2. Proposal of new method

2.1. PAT model and performance curves at various viscosities

The PAT model is a single-stage, end-suction experimental centrifugal pump with a specific speed of $n_{sp} = 3.65 n_p \sqrt{Q_p}/H_p^{3/4} = 93$(r/min, m^3/s,m) in [31]. At the design point, the pump flow rate, Q_p, head, H_p, and rotational speed, n_p, are 25 m^3/h, 8 m and 1450 r/min. The impeller eye and outlet diameters are 62 mm and 180 mm, the number of blades is 4, the exit blade angle is 20^o(the angle between blade camber line and the reverse direction of impeller rotation), the warp angle of blade is 140^o. The diameter of base circle of the volute is 190 mm, the volute width is 40 mm, and the cross-sectional area of its throat is 1440 mm^2.

As a PAT, the rotational direction is shown in Fig. 1(a), the pump head and hydraulic efficiency curves at reference condition (ν = 1cSt for water) are illustrated in Fig. 1(b) at n_p = 1485 r/min. likewise, the PAT head, output power and hydraulic efficiency curves at five viscosities (ν = 1, 24, 48, 90 and 120cSt) are demonstrated in Fig. 1(c) and (e) at a rotational speed n_t = 1485 r/min. It is intended that those data are utilized to establish a performance conversion method of PAT at any viscosity of liquid based on the reference performance in the pump mode. The further information regarding to CFD computational and flow models as well as detailed results can be found in [31].

2.2. New method

Four sketches are illustrated in Fig. 2 to present the head and hydraulic efficiency curves at a viscosity of ν = 1cSt for water in pump mode and those for a liquid with viscosity more viscous than water in turbine mode. In Fig. 2(a), the reference operational point is the BEP in the pump mode, whilst in Fig. 2(b)–(d) five working points, namely ZEP, 0.8BEP, BEP, 1.2BEP and maximum flow rate are specified.

At first, based on the performance data shown in Fig. 1(b)–(e), the following conversion factors of flow rate, head, output power and hydraulic efficiency are defined and calculated at ZEP, 0.8BEP, BEP and 1.2BEP and maximum flow rate points of PAT

$$\begin{cases} q_0 = Q_{t0}/Q_{p1w}, h_0 = H_{t0}/H_{p1w}, \lambda_0 = P_{t0}/\rho_w g Q_{p1w} H_{p1w}, \varepsilon_0 = \eta_{ht0}/\eta_{hp1w} & \text{ZEP} \\ q_{0.8} = Q_{t0.8}/Q_{p1w}, h_{0.8} = H_{t0.8}/H_{p1w}, \lambda_{0.8} = P_{t0.8}/\rho_w g Q_{p1w} H_{p1w}, \varepsilon_{0.8} = \eta_{ht0.8}/\eta_{hp1w} & \text{0.8BEP} \\ q_1 = Q_{t1}/Q_{p1w}, h_1 = H_{t1}/H_{p1w}, \lambda_1 = P_{t1}/\rho_w g Q_{p1w} H_{p1w}, \varepsilon_1 = \eta_{ht1}/\eta_{hp1w} & \text{BEP} \\ q_{1.2} = Q_{t1.2}/Q_{p1w}, h_{1.2} = H_{t1.2}/H_{p1w}, \lambda_{1.2} = P_{t1.2}/\rho_w g Q_{p1w} H_{p1w}, \varepsilon_{1.2} = \eta_{ht1.2}/\eta_{hp1w} & \text{1.2BEP} \\ q_{\max} = Q_{t\max}/Q_{p1w}, h_{\max} = H_{t\max}/H_{p1w}, \lambda_{\max} = P_{t\max}/\rho_w g Q_{p1w} H_{p1w}, \varepsilon_{\max} = \eta_{ht\max}/\eta_{hp1w} & \text{Maximum flow rate} \end{cases} \quad (1)$$

where $q_{0.8}$ and $q_{1.2}$ are related to q_1 with the relationships of $q_{0.8} = 0.8q_1$, $q_{0.8} = 1.2q_1$, but $q_{\max}$ =2.6145. Note that $\lambda_0 = \varepsilon_0 = 0$ is always kept.

Secondly, those conversion factors are correlated to impeller Reynolds number, obtaining relationships such as q_0(Re), h_0(Re), λ_0(Re), ε_0(Re), $q_{0.8}$(Re), $h_{0.8}$(Re), $\varepsilon_{0.8}$(Re), q_1(Re), h_1(Re), ε_1(Re),$q_{1.2}$(Re), $h_{1.2}$(Re), $\varepsilon_{1.2}$(Re), $q_{\max}$(Re), $h_{\max}$(Re) and $\varepsilon_{\max}$(Re).

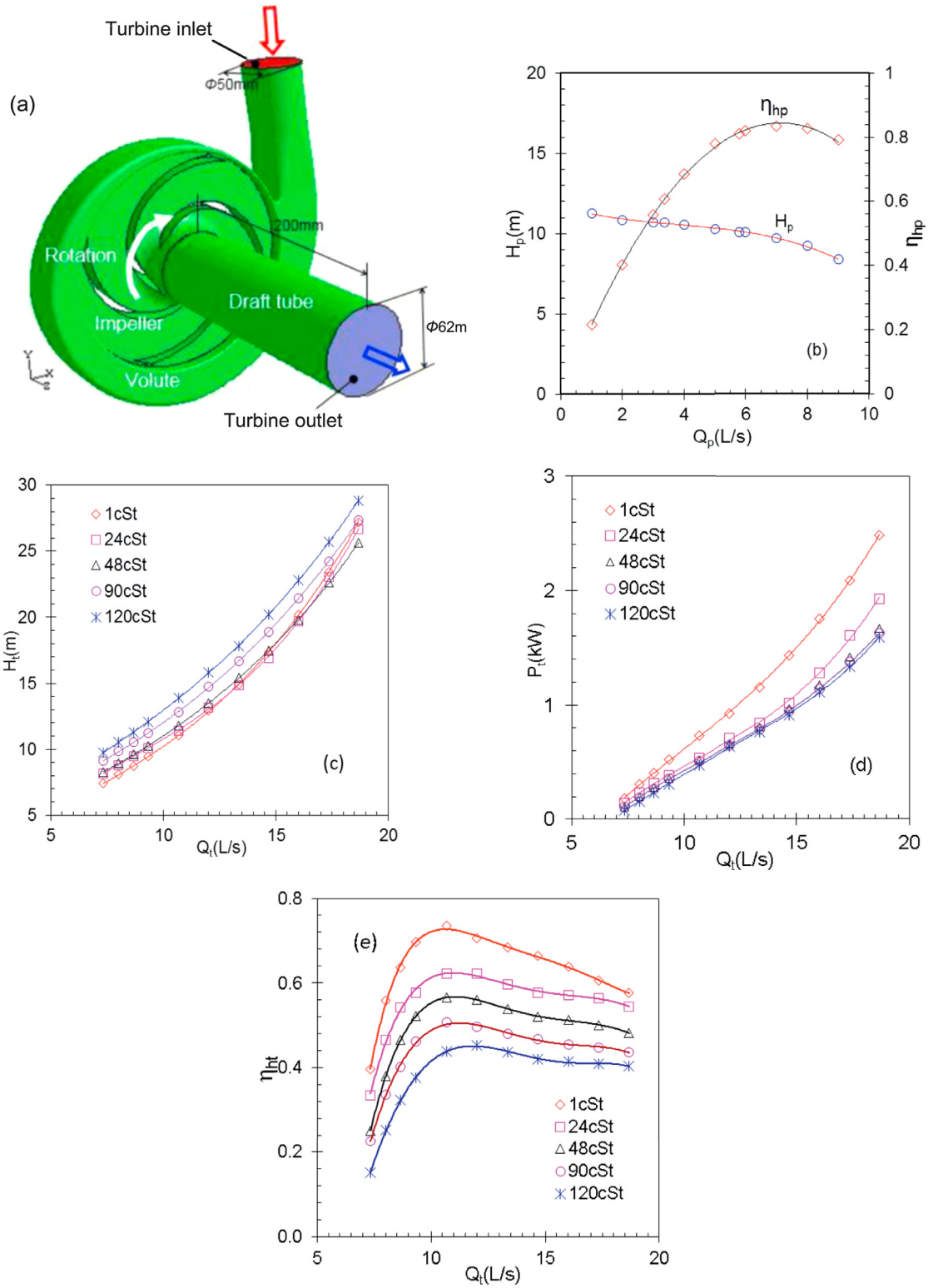

Fig. 1. Major geometrical dimensions and rotation direction of PAT, head and hydraulic efficiency curves in pump mode at 1cSt and head and hydraulic curves of PAT at various viscosities, (a) dimensions and rotation direction, (b) curves in pump mode, (c) head curves of PAT, (d) output power curves of PAT, (e) hydraulic efficiency curves of PAT.

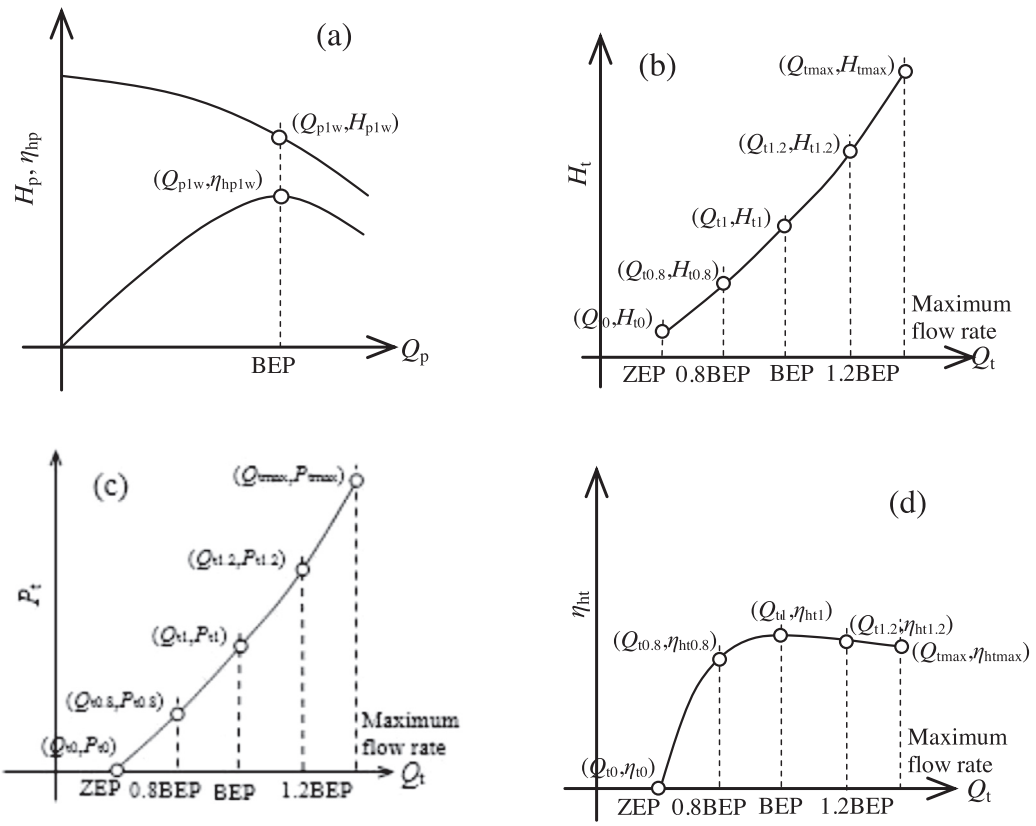

Fig. 2. Sketch of head and hydraulic efficiency curves in pump model at $\nu = 1$cSt for water and those in turbine mode at any viscosity of liquid, (a) pump mode, (b) turbine mode, the reference condition is BEP in the pump mode for water, five working conditions in the turbine mode are selected.

Then, we predict PAT performance curves at any viscosity or impeller Reynolds number by using those correlations and the performance parameters (Q_{p1w},H_{p1w}), and (Q_{p1w},η_{hp1w}) in the pump mode. In doing so, we need to calculate the PAT parameters Q_{t0}, H_{t0}, P_{t0} and η_{ht0} at ZEP, $Q_{t0.8}$, $H_{t0.8}$,$P_{t0.8}$ and $\eta_{ht0.8}$ at 0.8BEP, Q_{t1}, H_{t1}, P_{t1} and η_{ht1} at BEP, $Q_{t1.2}$, $H_{t1.2}$, $P_{t1.2}$ and$\eta_{ht1.2}$ at 1.2BEP as well as $Q_{t\max}$, $H_{t\max}$, $P_{t\max}$ and $\eta_{ht\max}$ at maximum flow rate by the following expressions

$$\begin{cases} Q_{t0} = q_0(\mathrm{Re})Q_{p1w},\ H_{t0} = h_0(\mathrm{Re})H_{p1w},\ P_{t0} = \lambda_0(\mathrm{Re})\rho_w g Q_{p1w}H_{p1w},\ \eta_{ht0} = \varepsilon_0(\mathrm{Re})\eta_{hp1w} & \text{ZEP} \\ Q_{t0.8} = q_{0.8}(\mathrm{Re})Q_{p1w},\ H_{t0.8} = h_{0.8}(\mathrm{Re})H_{p1w},\ P_{t0.8} = \lambda_{0.8}(\mathrm{Re})\rho_w g Q_{p1w}H_{p1w}, & \\ \quad \eta_{ht0.8} = \varepsilon_{0.8}(\mathrm{Re})\eta_{hp1w} & \text{0.8BEP} \\ Q_{t1} = q_1(\mathrm{Re})Q_{p1w},\ H_{t1} = h_1(\mathrm{Re})H_{p1w},\ P_{t1} = \lambda_1(\mathrm{Re})\rho_w g Q_{p1w}H_{p1w}, & \\ \quad \eta_{ht1} = \varepsilon_1(\mathrm{Re})\eta_{hp1w} & \text{BEP} \\ Q_{t1.2} = q_{1.2}(\mathrm{Re})Q_{p1w},\ H_{t1.2} = h_{1.2}(\mathrm{Re})H_{p1w},\ P_{t1.2} = \lambda_{1.2}(\mathrm{Re})\rho_w g Q_{p1w}H_{p1w}, & \\ \quad \eta_{ht1.2} = \varepsilon_{1.2}(\mathrm{Re})\eta_{hp1w} & \text{1.2BEP} \\ Q_{t\,\max} = q_{\max}(\mathrm{Re})Q_{p1w},\ H_{t\,\max} = h_{\max}(\mathrm{Re})H_{p1w},\ P_{t\,\max} = \lambda_{\max}(\mathrm{Re})\rho_w g Q_{p1w}H_{p1w}, & \\ \quad \eta_{ht\,\max} = \varepsilon_{\max}(\mathrm{Re})\eta_{hp1w} & \text{Maximum flow rate} \end{cases} \tag{2}$$

Finally, we can establish the PAT head curve and interpolate the heads at various flow rates by making use of a 4th order polynomial. The five coefficients of the polynomial, a_{H0} to a_{H4}, are decided by five points (Q_{t0},H_{t0}), ($Q_{t0.8}$,$H_{t0.8}$), (Q_{t1},H_{t1}), ($Q_{t1.2}$,$H_{t1.2}$) and ($Q_{t\max}$,$H_{t\max}$) by solving the following system of linear equations

$$\begin{cases} a_{H0} + a_{H1}Q_{t0} + a_{H2}Q_{t0}^2 + a_{H3}Q_{t0}^3 + a_{H4}Q_{t0}^4 = H_{t0} \\ a_{H0} + a_{H1}Q_{t0.8} + a_{H2}Q_{t0.8}^2 + a_{H3}Q_{t0.8}^3 + a_{H4}Q_{t0.8}^4 = H_{t0.8} \\ a_{H0} + a_{H1}Q_{t1} + a_{H2}Q_{t1}^2 + a_{H3}Q_{t1}^3 + a_{H4}Q_{t1}^4 = H_{t1} \\ a_{H0} + a_{H1}Q_{t1.2} + a_{H2}Q_{t1.2}^2 + a_{H3}Q_{t1.2}^3 + a_{H4}Q_{t1.2}^4 = H_{t1.2} \\ a_{H0} + a_{H1}Q_{t\,\max} + a_{H2}Q_{t\,\max}^2 + a_{H3}Q_{t\,\max}^3 + a_{H4}Q_{t\,\max}^4 = H_{t\,\max} \end{cases} \tag{3}$$

The hydraulic efficiency curves of PAT experience a sharp bend across the whole flow rate, as shown in Fig. 1(e). Consequently, utilising a 4th order polynomial to represent the curve usually results in an unsatisfactory curve-fitting. Alternatively, the output power curve can be established because of its simple shape, see Fig. 1(d). In that case, 3rd and 4th order polynomials have been tried, respectively. However, the curve fitting of the 4th order polynomial at five points (Q_{t0},P_{t0}), ($Q_{t0.8}$,$P_{t0.8}$), (Q_{t1},P_{t1}), ($Q_{t1.2}$,$P_{t1.2}$) and ($Q_{t\max}$,$P_{t\max}$) are poorer than with the 3rd order polynomial at four points ($Q_{t0.8}$,$P_{t0.8}$), (Q_{t1},P_{t1}), ($Q_{t1.2}$,$P_{t1.2}$) and ($Q_{t\max}$,$P_{t\max}$).

Bearing this in mind, the following system of linear equations is solved to specify four coefficients, a_{P0} to a_{P3}, of the 3rd order polynomial for the output power curve

$$\begin{cases} a_{P0.8} + a_{P1}Q_{t0.8} + a_{P2}Q_{t0.8}^2 + a_{P3}Q_{t0.8}^3 = P_{t0.8} \\ a_{P0} + a_{P1}Q_{t1} + + a_{P2}Q_{t1}^2 a_{P3}Q_{t1}^3 = P_{t1} \\ a_{P0} + a_{P1}Q_{t1.2} + a_{P2}Q_{t1.2}^2 + a_{P3}Q_{t1.2}^3 = P_{t1.2} \\ a_{P0} + a_{P1}Q_{t\max} + a_{P2}Q_{t\max}^2 + a_{P3}Q_{t\max}^3 = P_{t\max} \end{cases} \tag{4}$$

The systems of linear equations presented by Eqs. (3) and (4) are solved in MATLAB with *linsolve* function for unknowns a_{H0} to a_{H4} and a_{P0} to a_{P3}, respectively. Once these coefficients are available, we can adopt the following equations to interpolate head and output power and calculate hydraulic efficiency at any flow rate

$$\begin{cases} H_t = a_{H0} + a_{H1}Q_t + a_{H2}Q_t^2 + a_{H3}Q_t^3 + a_{H4}Q_t^4 \\ P_t = a_{P0} + a_{P1}Q_t + a_{P2}Q_t^2 + a_{P3}Q_t^3 \\ \eta_{ht} = P_t / \eta_{vt}\rho g H_t Q_t \end{cases} \tag{6}$$

at Q_{t0}, P_{t0} may not be exactly to zero, it should be enforced to be zero before calculating η_{ht}.

In [32], the side chambers between the impeller and the casing is excluded in CFD computational model, so the volumetric efficiency, η_{vt} remains unattainable in CFD simulations. Here it is assumed that the pump and turbine modes share a constant volumetric efficiency for all viscosity and working condition in CFD simulations, i.e. $\eta_{vt} = 0.8657$ [33].

Furthermore, the output power, P_t, in the third expression of Eq. (6) is just the power applied on the flow channels of impeller by the liquid rather than the output power on the shaft end of PAT. Consequently, the mechanical efficiency of PAT doesn't appear in the expression.

3. Results and discussion

3.1. Correlations of conversion factors

Four conversion factors at ZEP, 0.8BEP, BEP, 1.2BEP and maximum flow rate are illustrated in Fig. 3 in terms of impeller Reynolds number. For convenience of use, these factors have been correlated to impeller Reynolds number by curve-fitting technique in software Excel and presented as follows, namely at BEP

$$\begin{cases} q_1 = 1.4878 + 6.1500\times10^{-4}\left(\dfrac{\mathrm{Re}}{\mathrm{Re}_w}\right)^{-1.35} - 1.8617\times10^{-6}\left[\left(\dfrac{\mathrm{Re}}{\mathrm{Re}_w}\right)^{-1.35}\right]^2 + 2.0436\times10^{-9}\left[\left(\dfrac{\mathrm{Re}}{\mathrm{Re}_w}\right)^{-1.35}\right]^3 \\ h_1 = 1.0385 + 3.1531\times10^{-4}\left(\dfrac{\mathrm{Re}}{\mathrm{Re}_w}\right)^{-1.5} \\ \lambda_1 = 1.0995 - 1.4776\times10^{-1}\left(\dfrac{\mathrm{Re}}{\mathrm{Re}_w}\right)^{-0.4} + 1.5230\times10^{-2}\left[\left(\dfrac{\mathrm{Re}}{\mathrm{Re}_w}\right)^{-0.4}\right]^2 \\ \varepsilon_1 = 0.8879 - 2.4810\times10^{-2}\left(\dfrac{\mathrm{Re}}{\mathrm{Re}_w}\right)^{-0.55} \end{cases} \tag{7}$$

At 0.8BEP

$$\begin{cases} q_{0.8} = 0.8q_1 \\ h_{0.8} = 0.8086 + 1.0603\times10^{-3}\left(\dfrac{\mathrm{Re}}{\mathrm{Re}_w}\right)^{-1.2} \\ \lambda_{0.8} = 0.5285 - 1.3564\times10^{-2}\left(\dfrac{\mathrm{Re}}{\mathrm{Re}_w}\right)^{-0.7} + 3.8355\times10^{-4}\left[\left(\dfrac{\mathrm{Re}}{\mathrm{Re}_w}\right)^{-0.7}\right]^2 \\ \varepsilon_{0.8} = 0.7649 - 2.1506\times10^{-2}\left(\dfrac{\mathrm{Re}}{\mathrm{Re}_w}\right)^{-0.55} \end{cases} \tag{8}$$

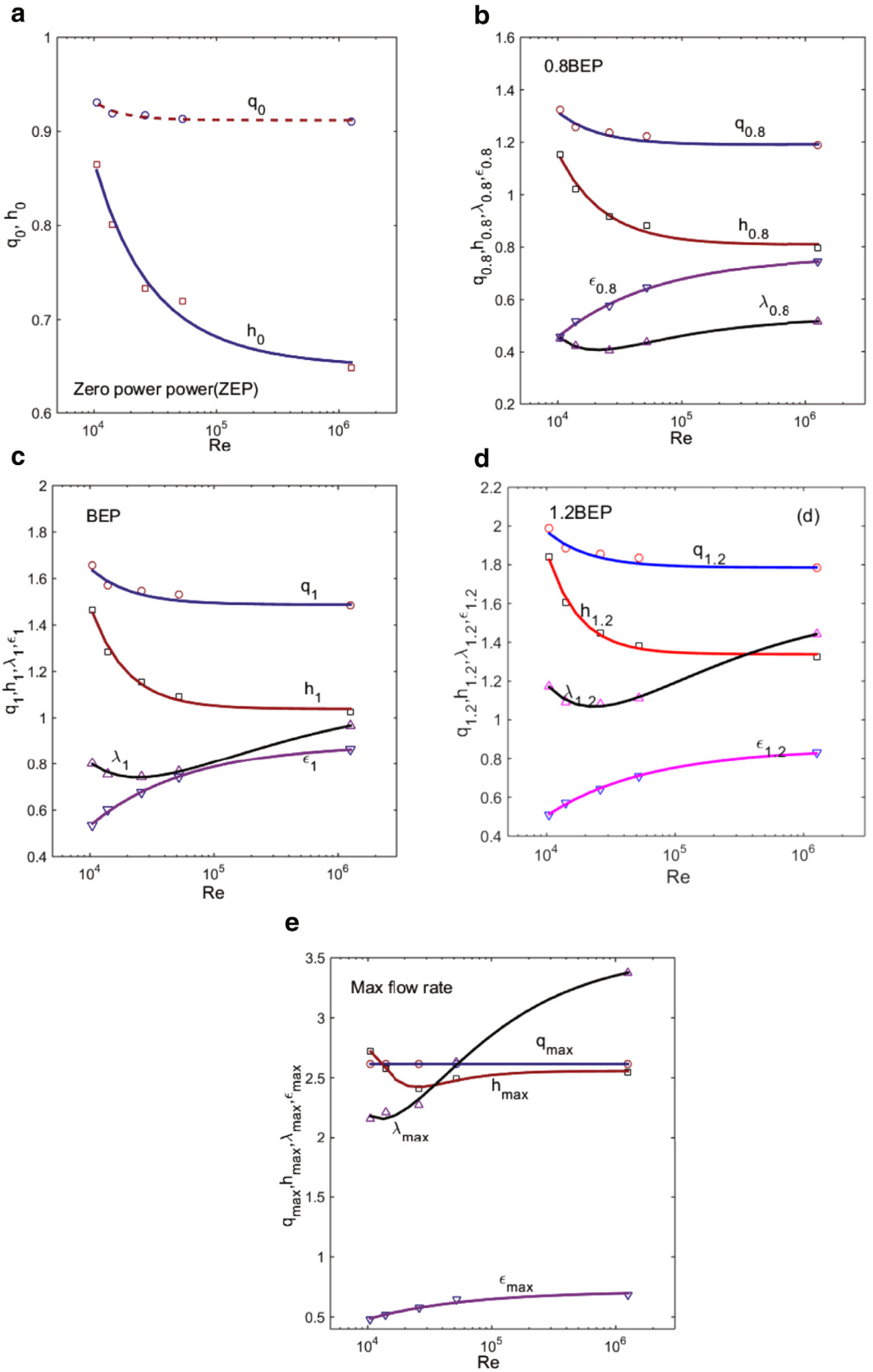

Fig. 3. Four conversion factors are in terms of impeller Reynolds number at ZEP, 0.8BEP, BEP, 1.2BEP and maximum flow rate.

Table 1
Density, kinematic viscosity of liquid and impeller Reynolds number at 20 °C.

Liquid	Density, ρ (kg/m^3)	Kinematic viscosity, ν (cSt or mm^2/s)	Impeller Reynolds number, Re
Water	998.2	1.0	1,259,622
Oil 1	839	24.0	52,484
Oil 2	851	48.0	26,242
Oil 3	861	90.0	13,996
Oil 4	865	120.0	10,497

At 1.2BEP

$$\begin{cases} q_{1.2} = 1.2q_1 \\ h_{1.2} = 1.3386 + 1.11786\times10^{-4}\left(\dfrac{\mathrm{Re}}{\mathrm{Re}_w}\right)^{-1.75} \\ \lambda_{1.2} = 1.6060 - 1.7900\times10^{-1}\left(\dfrac{\mathrm{Re}}{\mathrm{Re}_w}\right)^{-0.45} + 1.4881\times10^{-2}\left[\left(\dfrac{\mathrm{Re}}{\mathrm{Re}_w}\right)^{-0.45}\right]^2 \\ \varepsilon_{1.2} = 0.8510 - 2.4225\times10^{-2}\left(\dfrac{\mathrm{Re}}{\mathrm{Re}_w}\right)^{-0.55} \end{cases} \tag{9}$$

And at ZEP

$$\begin{cases} q_0 = 0.9102 + 4.4138\times10^{-5}\left(\dfrac{\mathrm{Re}}{\mathrm{Re}_w}\right)^{-1.45} - 8.5323\times10^{-8}\left[\left(\dfrac{\mathrm{Re}}{\mathrm{Re}_w}\right)^{-1.45}\right]^2 + 5.9605\times10^{-11}\left[\left(\dfrac{\mathrm{Re}}{\mathrm{Re}_w}\right)^{-1.45}\right]^3 \\ h_0 = 0.6496 + 4.9490\times10^{-3}\left[\left(\dfrac{\mathrm{Re}}{\mathrm{Re}_w}\right)^{-0.7}\right] + 8.3308\times10^{-5}\left[\left(\dfrac{\mathrm{Re}}{\mathrm{Re}_w}\right)^{-0.7}\right]^2 \\ \lambda_0 = 0 \\ \varepsilon_0 = 0 \end{cases} \tag{10}$$

And at maximum flow rate

$$\begin{cases} q_{\max} = 2.6145 \\ h_{\max} = 2.5573 - 8.4893\times10^{-4}\left(\dfrac{\mathrm{Re}}{\mathrm{Re}_w}\right)^{-1.5} + 1.5330\times10^{-6}\left[\left(\dfrac{\mathrm{Re}}{\mathrm{Re}_w}\right)^{-1.5}\right]^2 - 6.0354\times10^{-10}\left[\left(\dfrac{\mathrm{Re}}{\mathrm{Re}_w}\right)^{-1.5}\right]^3 \\ \lambda_{\max} = 3.5484 - 1.7803\times10^{-1}\left(\dfrac{\mathrm{Re}}{\mathrm{Re}_w}\right)^{-0.6} + 5.6936\times10^{-3}\left[\left(\dfrac{\mathrm{Re}}{\mathrm{Re}_w}\right)^{-0.6}\right]^2 \\ \varepsilon_{\max} = 0.7143 - 1.6243\times10^{-2}\left(\dfrac{\mathrm{Re}}{\mathrm{Re}_w}\right)^{-0.55} \end{cases} \tag{11}$$

where impeller Reynolds number is based on impeller inlet diameter, tip speed and liquid viscosity, $\mathrm{Re} = u_{1t}r_{1t}/\nu$, $u_{1t} = 14$ m/s, $r_{1t} = 0.09$ m and the reference Reynolds number $\mathrm{Re}_w = 1{,}259{,}622$ for water, see Table 1.

It is seen that the four performance conversion factors are largely dependent on working condition and impeller Reynolds number, especially for the head, power and hydraulic efficiency conversion factors. In particular, a higher flow rate leads to a larger flow rate, head and output power conversion factors. For the hydraulic efficiency conversion factor, however, the maximum value is arrived at BEP because the efficiency is the best there.

There is a monotonous relationship between hydraulic efficiency conversion factor and Reynolds number. Unfortunately, this is not true for the flow rate, head and power conversion factors, for example, three factors can be a 2nd or 3rd order polynomial in terms of Reynolds number, as shown in Eqs. (7)–(11).

3.2. PAT performance prediction with conversion factors

The PAT performance curves have been predicted by the above conversion factor correlations and compared with CFD results in Fig. 4. The head, output power and hydraulic efficiency curves given by conversion factor correlations illustrate quite good agreement with the performance curves predicted with CFD at five viscosities, suggesting the correlations proposed are viable.

To identify the accuracy of prediction of the correlations, the dimensionless root-mean-square errors (RMSE) are tabulated in Table 2. Those errors are defined by the following expressions

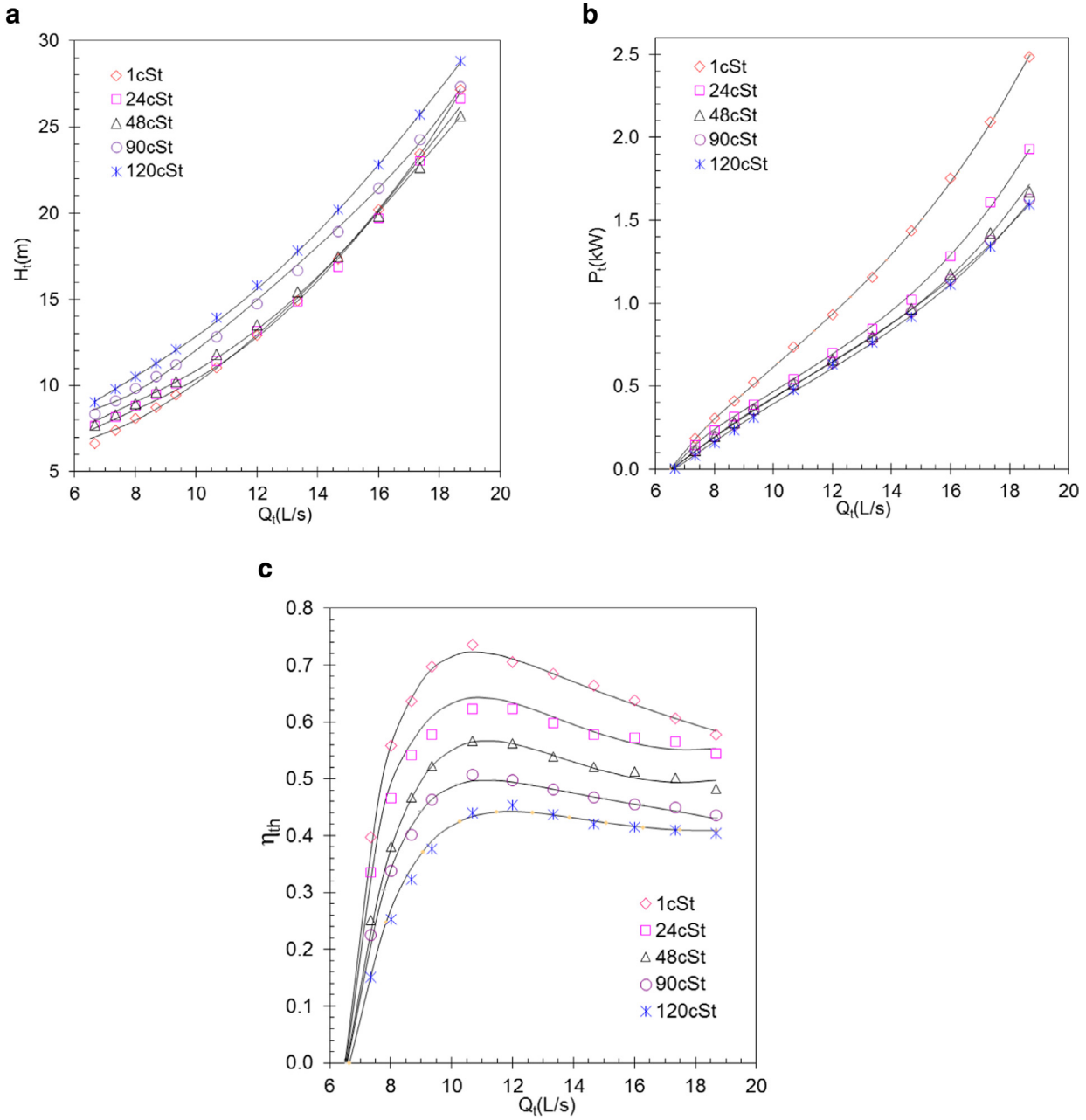

Fig. 4. Comparison of PAT head, output power and hydraulic efficiency curves predicted by CFD method and conversion factors model at five viscosities, (a) head, (b) output power, (c) hydraulic efficiency, the symbols for the data predicted by CFD, the lines for the results based on conversion factors model.

Table 2
Errors between CFD results and predictions with conversion factors.

ν(cSt)	1	24	48	90	120
δ_H(%)	0.83	1.67	1.09	1.33	0.54
δ_P(%)	2.09	2.18	2.57	2.44	1.19
δ_η(%)	3.97	6.76	2.27	3.31	2.56

$$\begin{cases} \delta_H = \dfrac{\sqrt{\sum_{i=1}^{m}\left(H_{t,i}^{CFD} - H_{t,i}^{\mathrm{mod}}\right)^2}}{H_{t1}} \times 100\% \\ \delta_P = \dfrac{\sqrt{\sum_{i=1}^{m}\left(P_{t,i}^{CFD} - P_{t,i}^{\mathrm{mod}}\right)^2}}{P_{t1}} \times 100\% \\ \delta_\eta = \dfrac{\sqrt{\sum_{i=1}^{m}\left(\eta_{ht,i}^{CFD} - \eta_{ht,i}^{\mathrm{mod}}\right)^2}}{\eta_{ht1}} \times 100\% \end{cases} \tag{12}$$

The errors in prediction of head, output power and hydraulic efficiency are equal to or less than 1.67%, 2.57% and 6.76%, respectively. The best accuracy in the head is achieved, but the poorest exists in the hydraulic efficiency. Specially, at 24cSt, the error in the head is the largest in curve-fitting, causing the poorest representation of hydraulic efficiency curve. The results above clearly demonstrate the conversion factors model proposed are reasonable and accurate.

3.3. Conversion factors for hydraulic loss and impeller theoretical head

Hydraulic loss and impeller theoretical head of PAT may be important in its performance analysis. Similar to the definition of hydraulic performance conversion factors in Section 2.2, PAT hydraulic loss and impeller theoretical head conversion factors are defined by the follow expressions at 0.8BEP, BEP and 1.2BEP, respectively

$$\begin{cases} \kappa_{0.8} = H_{Lt0.8}/H_{Lp1w}, \kappa_1 = H_{Lt1}/H_{Lp1w}, \kappa_{1.2} = h_{Lt1.2}/H_{Lp1w} \\ h_{e0.8} = H_{et0.8}/H_{ep1w}, h_{e1} = H_{et1}/H_{ep1w}, h_{e1.2} = H_{et1.2}/H_{ep1w} \end{cases} \tag{13}$$

These conversion factors can be correlated to impeller Reynolds number as well like the following expressions

$$\begin{cases} \kappa_{0.8} = 2.2409 + 1.1353 \times 10^{-1}\left(\dfrac{\mathrm{Re}}{\mathrm{Re}_w}\right)^{-0.55} \\ \kappa_1 = 1.5917 + 1.3097 \times 10^{-1}\left(\dfrac{\mathrm{Re}}{\mathrm{Re}_w}\right)^{-0.55} \\ \kappa_{1.2} = 1.7864 + 1.2788 \times 10^{-1}\left(\dfrac{\mathrm{Re}}{\mathrm{Re}_w}\right)^{-0.55} \end{cases} \tag{14}$$

And

$$\begin{cases} h_{e0.8} = 0.7921 - 1.0914 \times 10^{-3}\left(\dfrac{\mathrm{Re}}{\mathrm{Re}_w}\right)^{-0.9} + 5.9802 \times 10^{-6}\left[\left(\dfrac{\mathrm{Re}}{\mathrm{Re}_w}\right)^{-0.9}\right]^2 - 6.9254 \times 10^{-7}\left[\left(\dfrac{\mathrm{Re}}{\mathrm{Re}_w}\right)^{-0.9}\right]^3 \\ h_{e1} = 0.9155 - 4.0198 \times 10^{-2}(\mathrm{Re}/\mathrm{Re}_w)^{-0.25} \\ h_{e1.2} = 0.6473 + 1.0599\left(\dfrac{\mathrm{Re}}{\mathrm{Re}_w}\right)^{-0.15} - 9.4624 \times 10^{-1}\left[\left(\dfrac{\mathrm{Re}}{\mathrm{Re}_w}\right)^{-0.15}\right]^2 + 2.3495 \times 10^{-1}\left[\left(\dfrac{\mathrm{Re}}{\mathrm{Re}_w}\right)^{-0.15}\right]^3 \end{cases} \tag{15}$$

These two conversion factors are illustrated in Fig. 5. The hydraulic efficiency and loss conversion factors share an identical power -0.55, suggesting two factors are equal in physical meaning. The hydraulic loss conversion factor declines with decreasing Reynolds number, and it is the maximum at 0.8BEP, and the minimum at BEP.

The impeller theoretical head conversion factors show a complex relation with impeller Reynolds number at 0.8BEP and 1.2BEP. However, the factor at BEP is simple and just drops off with decreasing Reynolds number. Such variation features in the theoretical head conversion factors well reflect the behaviour of the theoretical head curves in terms of flow rate at various viscosities, as shown in Fig. 5(c). The impeller theoretical head is basically decided by the flow pattern at the volute outlet of PAT, particularly the circumferential component of fluid velocity [32].

3.4. Comparison with existing conversion factors

There are various empirical correlations of flow rate, head and efficiency conversion factors at BEP in literature, see Appendix A for details. They can be classified into four categories: (a) constant factors, (b) as a function of specific speed in pump mode, (c) as a function of efficiency in pump mode, (d) as a function of both specific speed and efficiency in pump. The flow rate, head and hydraulic efficiency conversion factors at BEP presented by Eq. (7) are compared with those expressed by Eqs. (A1)–(A16) in Appendix A in Figs 6–9.

To work out the conversion factors with Eqs. (A3)–(A7), (A11)–(A16), the pump efficiency is estimated by $\eta_p = \eta_{ht}\eta_{vt}\eta_{mt}$, where the volumetric efficiency $\eta_{vp} = 0.8657$ and the mechanical efficiency $\eta_{mp} = 0.8964$ at 1cSt [33], η_{ht} is illustrated in Fig. 1(e).

The flow rate conversion factors predicted with the formulas developed by Palgrave, Williams, Yang et al, Gopalakrishnan, Derakhshan & Nourbakhsh, Singh & Nestmann, respectively, show good agreement with that in the present paper.

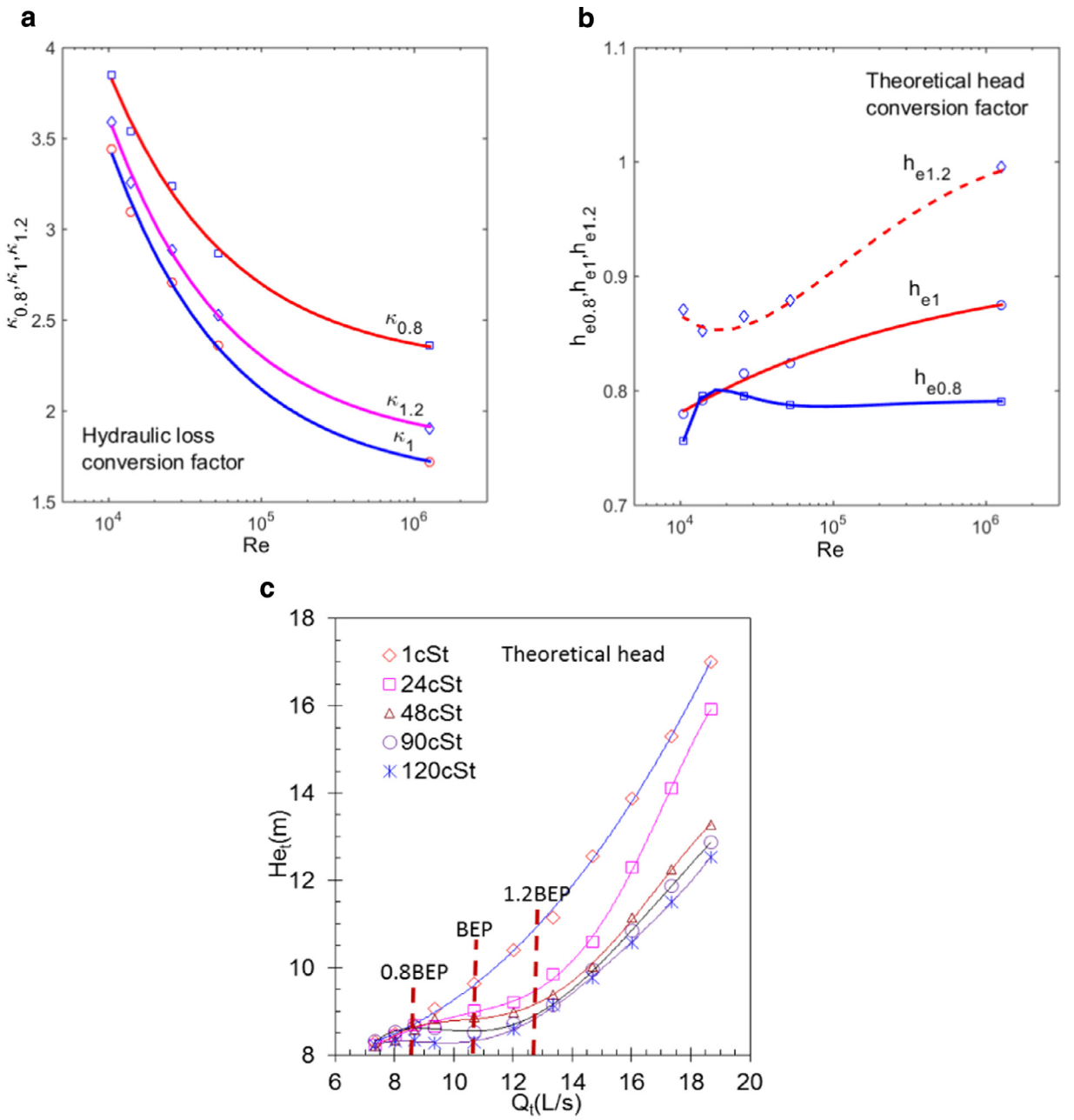

Fig. 5. Hydraulic loss and theoretical head conversion factors as a function of impeller Reynolds number at 0.8BEP, BEP and 1.2BEP as well as PAT theoretical head variation in terms of flow rate, '0.8BEP, BEP and 1.2BEP' is for 1cSt viscosity.

The hydraulic efficiency conversion factors estimated with the expressions proposed by Grover, Derakhshan & Nourbakhsh, Singh & Nestmann agree well with the factor proposed in the paper.

The head conversion factors from the existing formulas show a significant difference from that originated from CFD simulations here. This is because pump blade geometrical and specific speed have significant effects on the conversion factor and a general correlation cannot fit every special pump case.

To clarify the pump blade geometrical and specific speed effects on the conversion factors, the flow rate, head and hydraulic conversion factors of two additional centrifugal pumps have been extracted at BEP based on corresponding CFD results with the same methodlogy used in the paper. The first centrifugal pump with a specific speed, $n_{sp}=93$, has the same volute and impeller geometry as well as rotational speed, but the exit blade angle is $\beta_{2p} = 44^{o}$, shown in Fig. 10(a), as the pump in this paper. The performance and fluid flow of centrifugal pumps with these two kinds of exit blade angles have

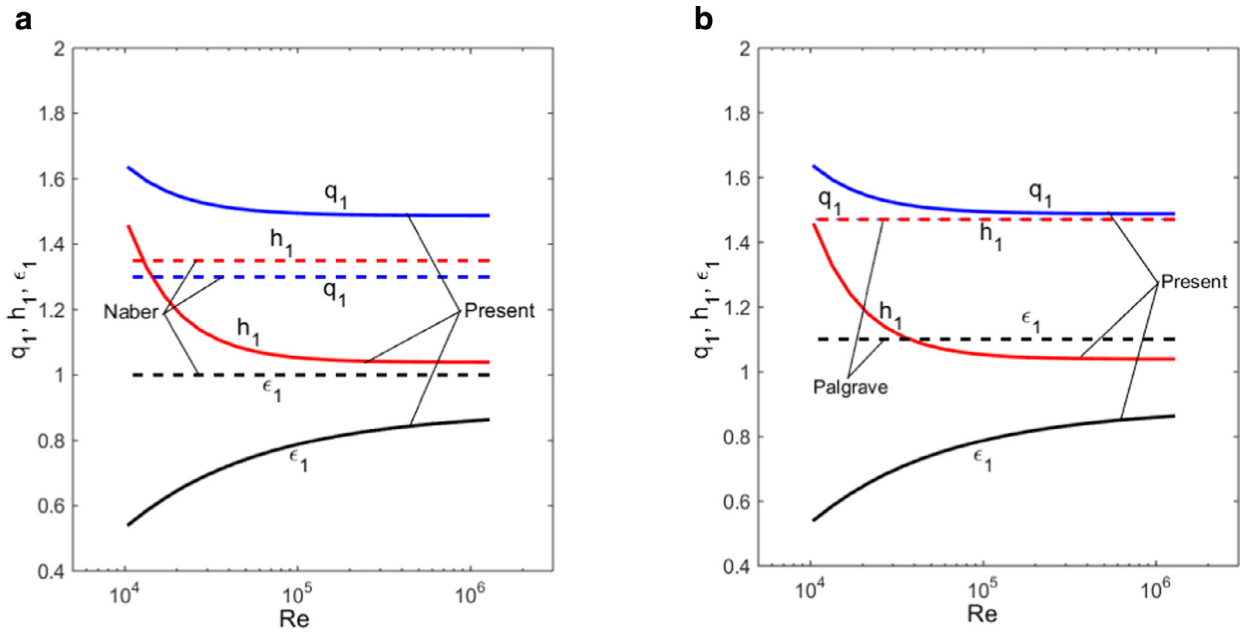

Fig. 6. Comparison of conversion factors between CFD prediction and empirical correlations proposed by Naber and Palgrave, respectively.

been detailed experimentally and numerically at various viscosities of liquid in [34]. The obtained correlations for the three conversion factors are as follows

$$\begin{cases} q_1 = 1.9811 + 4.9341 \times 10^{-4}\left(\dfrac{\mathrm{Re}}{\mathrm{Re}_w}\right)^{-1.5} - 1.7444 \times 10^{-7}\left[\left(\dfrac{\mathrm{Re}}{\mathrm{Re}_w}\right)^{-1.5}\right]^2 \\ h_1 = 1.9701 + 5.1938 \times 10^{-4}\left(\dfrac{\mathrm{Re}}{\mathrm{Re}_w}\right)^{-1.5} - 2.0807 \times 10^{-7}\left[\left(\dfrac{\mathrm{Re}}{\mathrm{Re}_w}\right)^{-1.5}\right]^2 \\ \varepsilon_1 = 0.9116 - 2.7058 \times 10^{-2}\left(\dfrac{\mathrm{Re}}{\mathrm{Re}_w}\right)^{-0.55} \end{cases} \tag{16}$$

and are plotted in Fig. 10(c) as a function of $\mathrm{Re}/\mathrm{Re}_w$.

The second centrifugal pump, shown in Fig. 10(b), is a high specific speed pump of $n_{sp}=207$ with a duty point, such as 106.8m^3/h flow rate, 18 m head and 2880r/min rotational speed, and 135.1 mm diameter, 30° exit blade angle and 22.5 mm outlet blade, see [35]. The turbine performance of the pump has been investigated at different viscosities by using the same method used in this paper with a set of meshes (40,260 hexahedral cells in the discharge nozzle, 224,746 hybrid cells in the impeller, 513,481 hybrid cells in the volute and 78,660 hexahedral cells in the suction pipe). The fitted correlations for the three conversion factors are the following

$$\begin{cases} q_1 = 1.4643 + 1.0886 \times 10^{-3}\left(\dfrac{\mathrm{Re}}{\mathrm{Re}_w}\right)^{-1.15} - 1.6776 \times 10^{-6}\left[\left(\dfrac{\mathrm{Re}}{\mathrm{Re}_w}\right)^{-1.15}\right]^2 \\ h_1 = 1.3281 + 2.4896 \times 10^{-3}\left(\dfrac{\mathrm{Re}}{\mathrm{Re}_w}\right)^{-1.15} - 4.9515 \times 10^{-6}\left[\left(\dfrac{\mathrm{Re}}{\mathrm{Re}_w}\right)^{-1.15}\right]^2 \\ \varepsilon_1 = 0.9562 - 1.1391 \times 10^{-2}\left(\dfrac{\mathrm{Re}}{\mathrm{Re}_w}\right)^{-0.55} \end{cases} \tag{17}$$

and are plotted in Fig. 10(c) as a function of $\mathrm{Re}/\mathrm{Re}_w$ as well. For this pump, the Reynolds number of for pumping water is 1,376,169.11.

Based on Fig. 10(c), the hydraulic efficiency conversion factor shows a less variation with blade exit angle and pump specific speed than the flow rate and head conversion factors. The hydraulic efficiency is less affected by the viscosity of liquid in turbine mode for the pump with the higher specific speed. The width of blade of a centrifugal pump with higher specific speed is wider than the pump with lower specific speed, suggesting the impeller and volute with a larger hydraulic diameter. Further, the length of blade of a centrifugal pump with higher specific speed is shorter as well. These two facts indicate the liquid experience a less flow resistance in the flow passages. As a result, the hydraulic efficiency conversion factor changes slightly with Reynolds number.

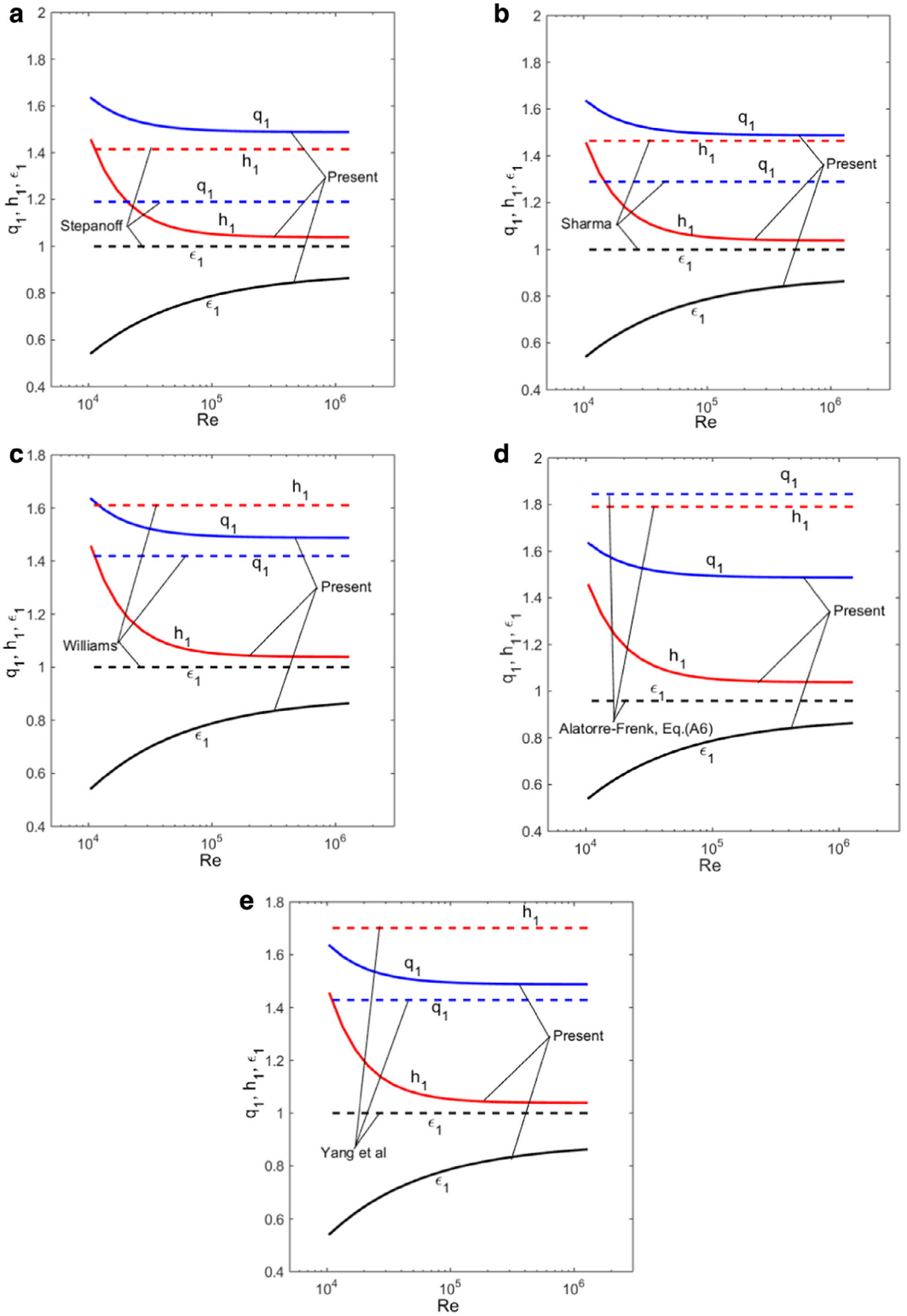

Fig. 7. Comparison of conversion factors between CFD prediction and empirical correlations proposed by Stepanoff, Sharma, Williams and Alatorre-Frenk, Eq. (A6).

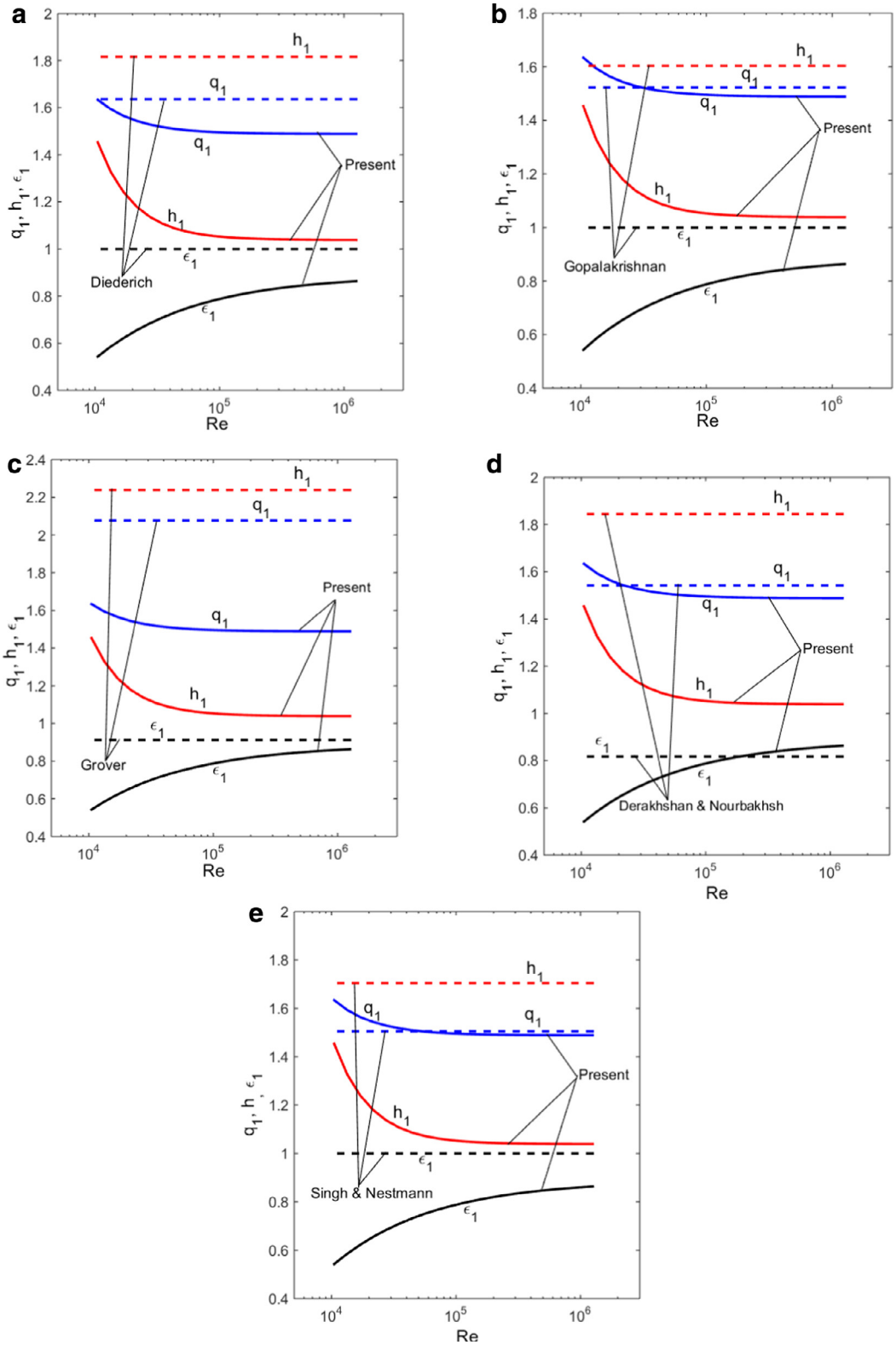

Fig. 8. Comparison of conversion factors between CFD prediction and empirical correlations proposed by Diederich, Gopalakrishann, Grover, Nautiyal et al and Singh & Nestmann in terms of specific speed.

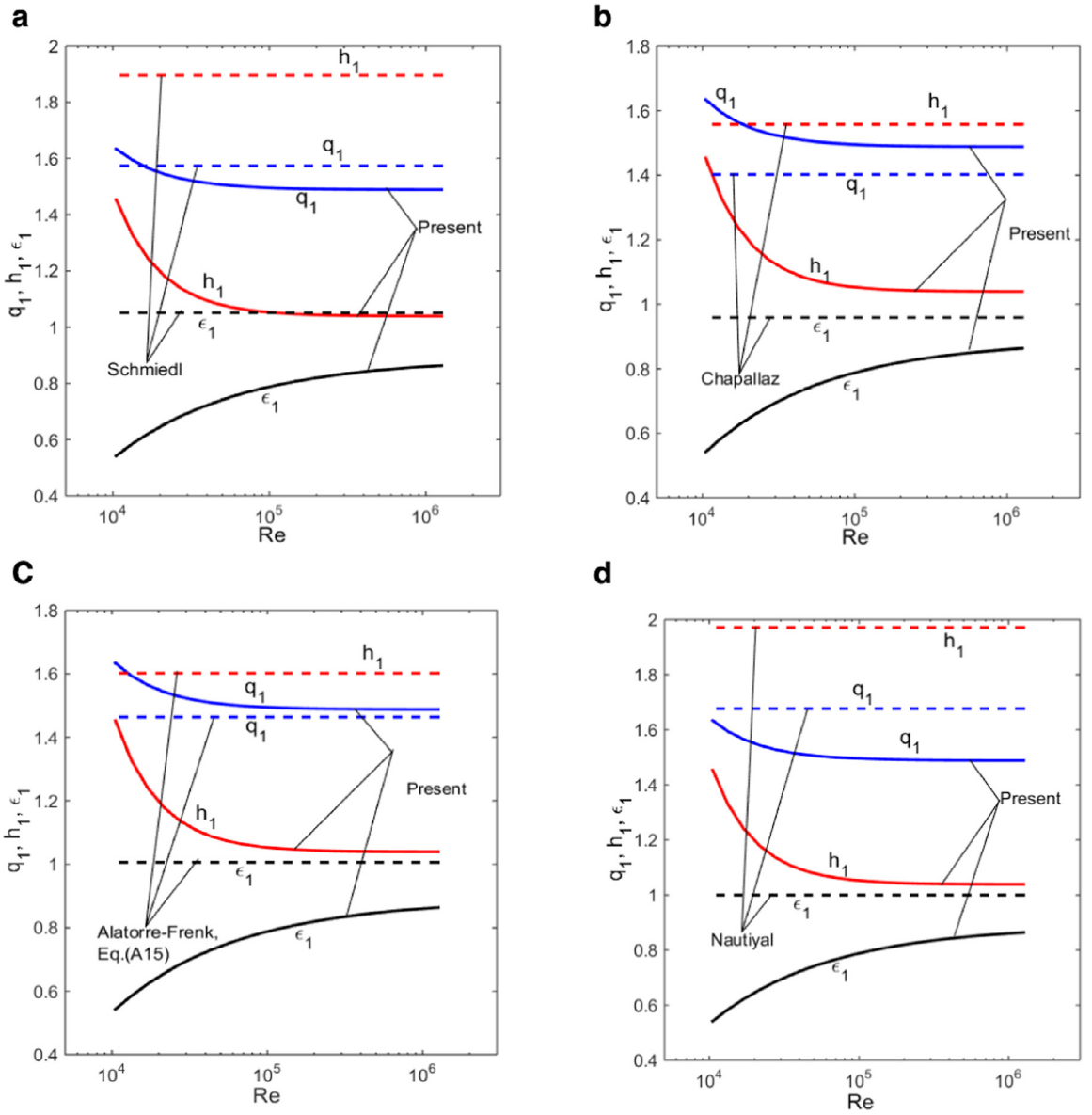

Fig. 9. Comparison of conversion factors between CFD prediction and empirical correlations proposed by Schmiedl, Chapallaz and Alatorre-Frenk in terms of specific speed and pump efficiency.

For the flow rate and head conversion factors, the effects of exit blade angle and specific speed are substantial. At the same specific speed, a larger exit blade angle can result in a bigger flow rate or head conversion factor. It seems that a high specific speed centrifugal pump possesses small flow rate and head conversion factors. To have a clear picture of this, the effect of specific speed on three conversion factors will be clarified in detail in the next section.

Centrifugal pumps in a variety of specific speeds and blade geometries can operate as turbine, and their three conversion factors depend upon both specific speed and blade geometry presented above, thus the investigations into the correlation of three conversion factors with Reynolds number, specific speed and blade geometry have to persist for a long time in the future. The factors expressed in Eq. (7) is just a special case, unlikely universal.

3.5. New correlations of conversion factors

To improve the accuracy of existing PAT flow rate, head and efficiency conversion factors at BEP, PAT performance data have been searched in literature and summarised in Table 3. The three conversion factors have been correlated to both

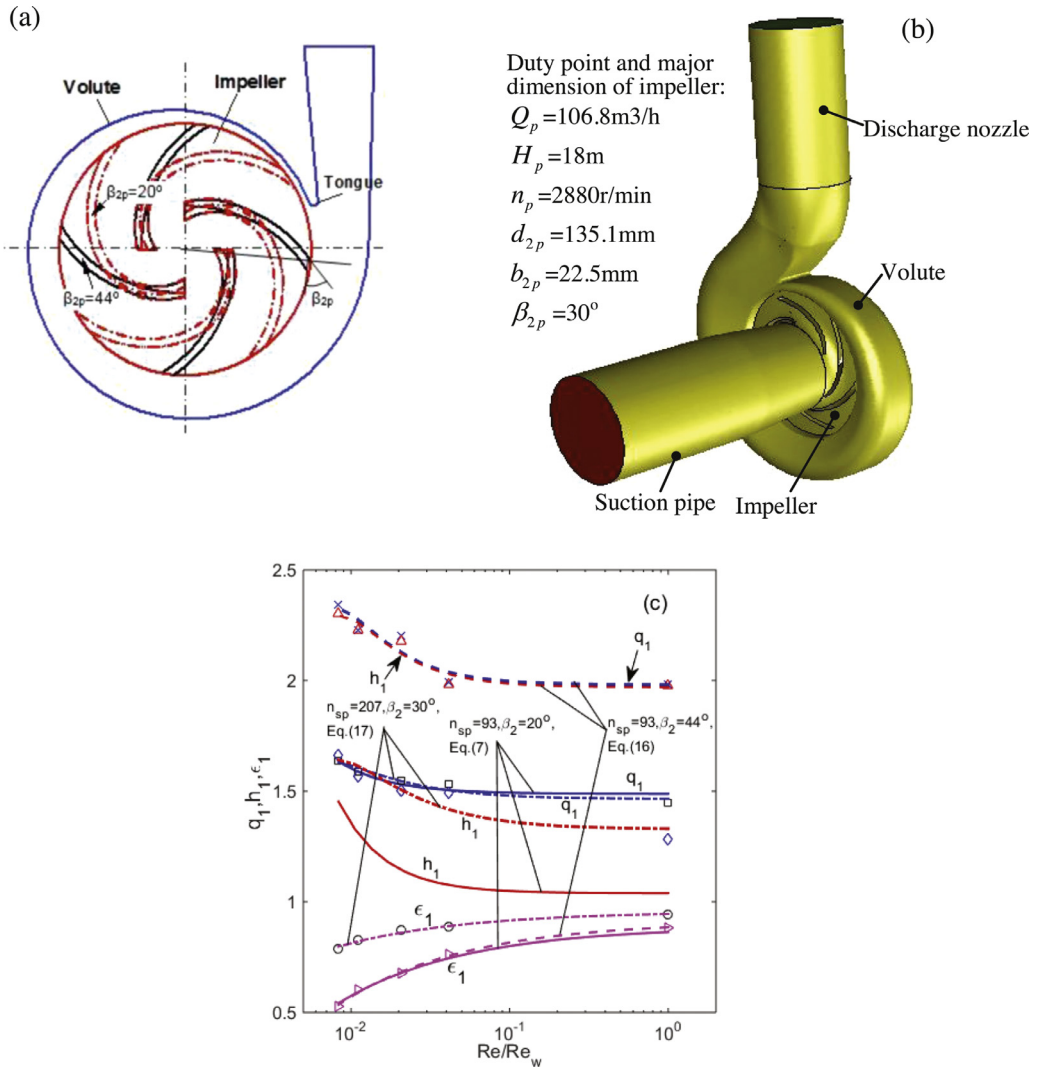

Fig. 10. Two centrifugal pumps and their flow rate, head and hydraulic efficiency conversion factors at BEP, (a) two impellers of a centrifugal pump of specific speed n_{sp} = 93 with the same geometrical dimensions except blade shape and exit blade angle, β_{2p}, the impeller with β_{2p} = 44o is after [34], (b) a centrifugal pump with a specific speed, n_{sp} = 207, from [35].

specific speed and pump efficiency as follows

$$\begin{cases} q_1 = 1.9597 - 0.5701\left(\eta_{p1}^2 N_{p1}^{0.1}\right) \\ h_1 = 2.6381 - 1.1524\left(\eta_{p1}^2 N_{p1}^{0.1}\right) \\ \varepsilon_1 = 0.9984 - 2.6804 \times 10^{-2}\left(\eta_{p1}^2 N_{p1}^{0.1}\right) \end{cases} \tag{18}$$

To illustrate their tendency of variation with specific speed, the three conversion factors are plotted in Fig. 11 along with the factors predicted by Alatorre-Frenk correlation Eq. (A15) and Nautiyal et al formula Eq. (A16). The scattered data points presented in Table 3 are involved in the figure as well. Because Eq. (18) entirely and Eq. (A15) partially are based on these data points, the factors from two equations are basically in agreement with the data points. The fluctuation in the curves represents the influence of pump efficiency on the factors. Unfortunately, the curves predicted by Eq. (A16) demonstrate a huge fluctuation, suggesting this correlation is not applicable for this series of data points.

If the efficiency effect on the factors is ignored, the flow rate, heat and efficiency conversion factors can be represented by a logarithmic function of specific speed, and the corresponding correlations have been depicted in Fig. 11(a)–(c). It is observed that three conversion factors rise with reducing pump specific speed, especially for the flow rate and head conversion factors.

Note that the behaviour of the correlation of Chapallaz Eq. (A14) with specific speed is quite similar to the Alatorre-Frenk formula Eq. (A15), and is no longer discussed.

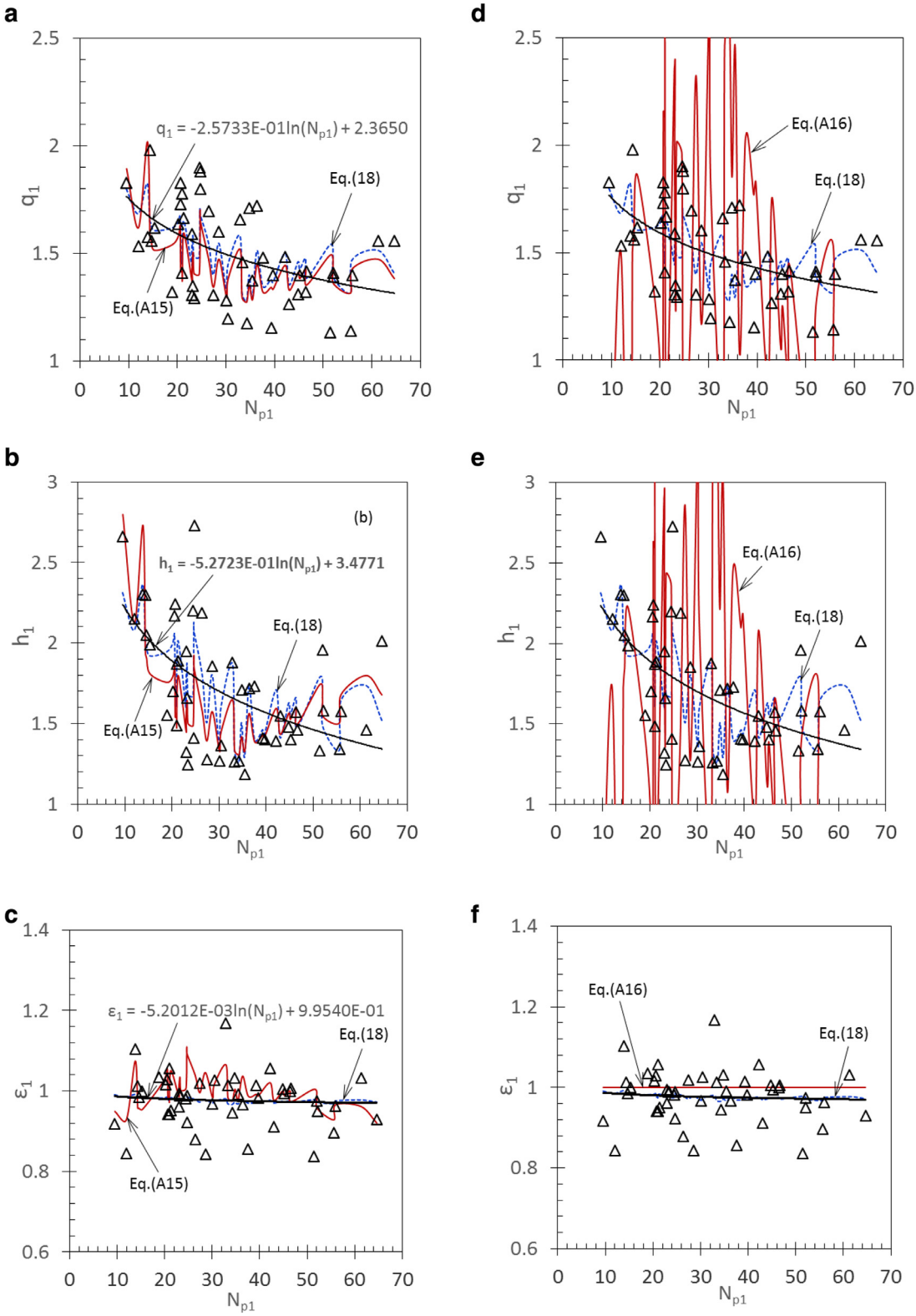

Fig. 11. Effects of pump specific speed and efficiency on conversion factors, the curves stand for the factors predicted by using various empirical correlations, the symbols are for the scattered data point in Table 3.

Table 3
PAT performance conversion factors of existing end-suction centrifugal pumps.

No	N_p	Q_p(m^3/s)	η_p	q_1	h_1	ε_1	Re	Source
1	9.55	5.5100E–03	0.4740	1.8276	2.6632	0.9177	3141,593	[11]
2	11.98	1.2530E–02	0.6150	1.5333	2.1518	0.8439	2466,360	
3	13.83	2.2260E–03	0.4260	1.5776	2.3015	1.1033	1457,270	
4	14.35	8.7000E–03	0.6450	1.9800	2.2969	1.0124	1636,246	
5	14.60	1.3000E–03	0.6500	1.5600	2.0500	0.9846	2372,557	
6	15.32	3.0620E–02	0.6880	1.6176	1.9874	1.0000	8295,768	
7	18.90	1.0710E–02	0.6690	1.3203	1.5536	1.0344	2010,619	
8	20.22	6.9400E-03	0.6400	1.6380	1.7004	1.0156	1499,010	
9	20.59	5.2120E–02	0.6115	1.8271	2.1677	1.0294	2553,526	[36]
10	20.70	3.5000E–02	0.7700	1.7300	2.2400	0.9416	971,799	[18]
11	21.00	1.0800E–02	0.7700	1.7800	1.8700	0.9416	1988,039	[16]
12	21.01	1.0000E–03	0.8080	1.4090	1.4870	1.0569	285,109	[11]
13	21.31	5.1710E–02	0.6308	1.6658	1.8870	0.9509	2168,681	[36]
14	22.99	5.1390E–02	0.8100	1.3053	1.3198	0.9938	4380,794	[11]
15	23.00	2.3000E–02	0.7600	1.5900	1.9500	0.9605	2372,557	[18]
16	23.23	1.0000E–03	0.6950	1.3491	1.6590	0.9884	276,938	[11]
17	23.41	8.4400E–02	0.7780	1.2927	1.2439	0.9884	5972,293	
18	24.50	3.4000E–02	0.7800	1.9000	2.2000	0.9808	2613,962	[16]
19	24.69	9.8600E–03	0.5690	1.7998	1.4073	0.9227	2659,044	[11]
20	24.71	4.9800E–02	0.5955	1.8801	2.7287	0.9881	1815,251	[36]
21	26.43	1.9420E–02	0.7210	1.6967	2.1877	0.8793	2094,395	[11]
22	27.41	1.0000E–03	0.8400	1.3050	1.2740	1.0190	1098,330	
23	28.57	1.0670E–02	0.7200	1.6026	1.8542	0.8431	1767,146	
24	30.10	1.0000E–03	0.8900	1.2825	1.2661	0.9674	6891,023	
25	30.44	4.3060E–02	0.8000	1.1955	1.3619	1.0263	2650,716	
26	32.89	8.5400E–03	0.6840	1.6581	1.8770	1.1681	811,459	
27	33.31	1.8320E–01	0.8930	1.4591	1.2605	1.0134	7566,002	
28	34.25	2.1070E–01	0.9180	1.1763	1.2664	0.9455	7697,145	
29	34.80	5.6000E–02	0.7850	1.7100	1.7100	1.0318	1518,436	[18]
30	35.46	1.9550E–01	0.9040	1.3724	1.1845	0.9912	7566,002	[11]
31	36.40	1.5300E–02	0.7400	1.7200	1.7200	0.9662	1149,305	[16]
32	37.60	5.7200E–02	0.8650	1.4800	1.7300	0.8555	2372,557	[18]
33	39.28	5.2530E–02	0.8410	1.1523	1.4073	1.0143	1473,010	[11]
34	39.70	6.5900E–02	0.8500	1.4000	1.4000	0.9824	2645,724	[16]
35	42.19	1.9621E–02	0.7440	1.4832	1.3910	1.0565	1186,278	[11]
36	43.01	4.2920E–02	0.8550	1.2646	1.5476	0.9111	1883,424	
37	44.80	8.6100E–02	0.7750	1.3092	1.4796	1.0052	3181,386	
38	45.20	3.3000E–02	0.8000	1.4000	1.4000	0.9938	1518,436	[16]
39	46.40	1.3500E–02	0.7600	1.3200	1.5700	1.0000	733,443	[16]
40	46.64	8.0500E–02	0.8290	1.4161	1.4579	1.0060	3509,486	[11]
41	51.44	1.3265E–02	0.7050	1.1308	1.3333	0.8369	1570,796	[24]
42	52.02	5.2100E–02	0.7570	1.3924	1.9574	0.9749	1672,148	[11]
43	52.13	2.1528E–02	0.8240	1.4100	1.5800	0.9500	716,807	[22]
44	55.60	1.0700E–01	0.8700	1.1400	1.3400	0.8966	2372,557	[18]
45	55.98	3.3800E–02	0.7580	1.3994	1.5772	0.9631	1640,383	[11]
46	61.30	2.8900E–02	0.7200	1.5600	1.4600	1.0319	1033,486	[16]
47	64.64	4.1670E–02	0.8000	1.5575	2.0116	0.9300	1120,010	[11]

For the relationships with impeller Reynolds number, the following expressions have been got

$$\begin{cases} q_1 = 1.5144 - 1.0557 \times 10^{-3}\left(\dfrac{\mathrm{Re}}{\mathrm{Re}_f}\right)^{-1.35} \\ h_1 = 1.5032 + 1.4343 \times 10^{-1}\left(\dfrac{\mathrm{Re}}{\mathrm{Re}_f}\right)^{-0.25} \\ \varepsilon_1 = 0.9065 + 4.8354 \times 10^{-2}\left(\dfrac{\mathrm{Re}}{\mathrm{Re}_f}\right)^{-0.25} \end{cases} \tag{19}$$

where the reference Reynolds number Re_f = 8,295,768 for centrifugal pump No.6. The conversion factors predicted with Eqs. (18) and (19) are compared in Fig. 12 with the factors obtained by CFD simulations. When Eq. (18) is employed to calculate the conversion factors of the pump in Section 2.1, the pump efficiency and specific speed have been involved in the equation. Also the Reynolds number scale in Table 3 is different from in Table 1, two Reynolds number ratios have to be

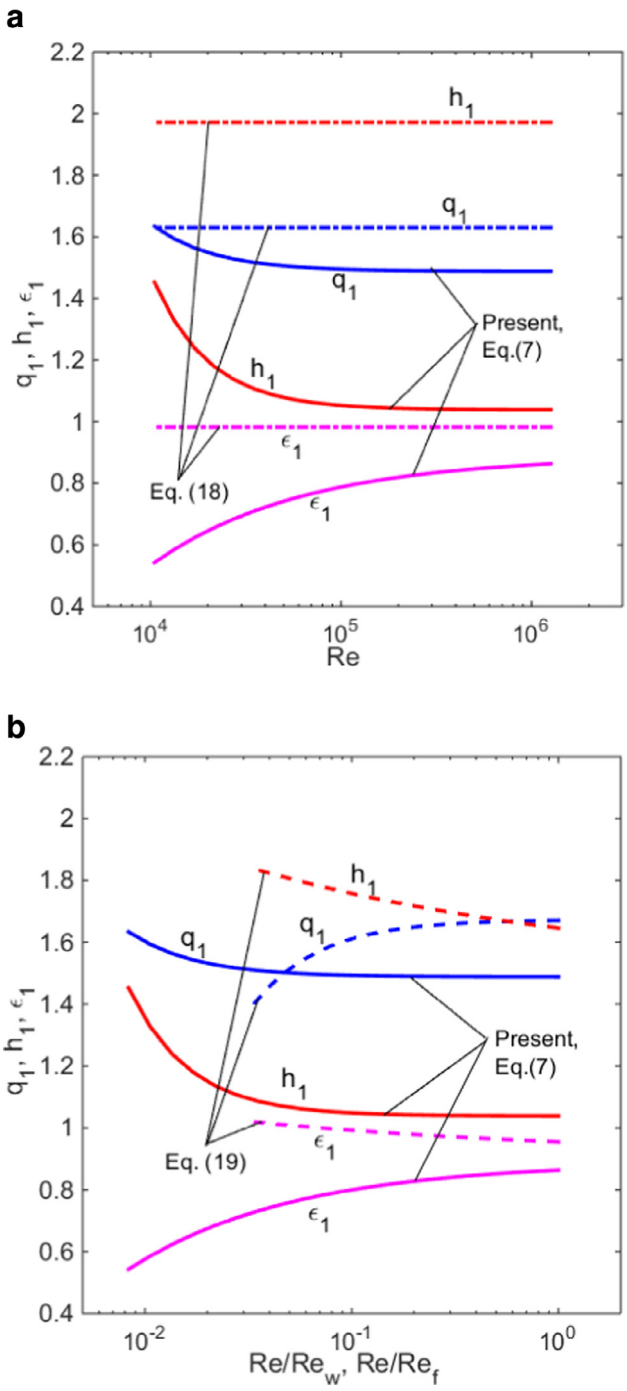

Fig. 12. Comparison of conversion factors between the CFD prediction Eq. (7) and the empirical correlations expressed as Eqs. (18) and (19).

considered in the abscissa in Fig. 12(b). For the correlations in Eq. (18), the predicted head and efficiency conversion factors still differ from CFD predictions considerably.

For the correlations in Eq. (19), even though Reynolds number effect has been involved, it doesn't seem strong enough to result in a significant change in the efficiency conversion factor when the number reduces. Note that an opposite variation tendency in the flow rate and efficiency conversion factors is predicted by Eq. (19) against the factors based on CFD prediction.

Honestly, when carrying out the curve-fitting for the correlations in Eq. (19), we just gathered the information of Reynolds number and three conversion factors of PATs with different specific speeds for water together. In that case, the obtained relationships between conversion factors and Reynolds number are subject to different meanings compared with

those for one PAT experiencing different Reynolds numbers, as shown in Section 3.1. Consequently, to clarify the effects of impeller Reynolds number on PAT conversion factors, PATs with different specific speeds should be measured and analysed at various viscosities of liquid in the future.

In the correlation model in the paper, one conversion factor is related to the output power acted on the inside impeller rather than on the shaft end, and on conversion factor is associated with the hydraulic efficiency, however, this model is a framework, naturally it is applicable for data reduction of experimental PAT performance curves as long as the output power on the shaft end and total efficiency are involved.

4. Conclusions

Based on a series of performance curves of a centrifugal pump as turbine obtained by CFD simulations at five viscosities, flow rate, head and output power and hydraulic efficiency conversion factors at zero efficiency/power, 0.8BEP, BEP, 1.2BEP and maximum flow rate points are defined and extracted. These factors have been correlated to impeller Reynolds number precisely. Relying on them, a performance conversion model in turbine mode from the pump mode is established by means of 3rd and 4th order polynomials for the output power and head curves. The flow rate, head and efficiency conversion factors have been compared with those found in literature. New correlations of flow rate, head and efficiency conversion factors are developed against specific speed as well as impeller Reynolds number. It is confirmed that the model can represent the performance curves in turbine mode with errors as low as 1.67%, 2.57% and 6.76% in head, output power and hydraulic efficiency curves, respectively. The present flow rate conversion factor agrees well with some existing empirical formulas, but the head and efficiency conversion factors don't. The new empirical formulas in connection with the performance data of pump as turbine in literature are in agreement with the present correlation of flow rate conversion factor, but they still are poorer in comparison with the head and efficiency conversion factors in the paper. This suggests that effects of impeller Reynolds number should receive considerable attention in the future.

Acknowledgement

Dr Yuliang, Zhang, who is associate professor in the school of Mechanical Engineering, Quzhou University in China, provided the geometrical model of the centrifugal pump with specific speed $n_{sp}=207$, and was appreciated very much.

Appendix A. Summary of conversion factors of pump as turbine

The performance conversion factors from pump mode to turbine mode can be divided into four groups, namely constant conversion factors, conversion factors in terms of pump hydraulic efficiency alone, conversion factors in terms of specific speed and those in terms of both hydraulic efficiency and specific speed [11].

In the first group, three conversion factors are constant. Naber put the following formulas forward for three conversion factors [11]

$$\begin{cases} q_1 = 1.3 \\ h_1 = 1.35 \\ \varepsilon_1 = 1 \end{cases} \tag{A1}$$

Later, Palgrave proposed the following expressions for the factors [11]

$$\begin{cases} q_1 = 1.471 \\ h_1 = 1.471 \\ \varepsilon_1 = 1.1 \end{cases} \tag{A2}$$

In the second group, the three conversion factors are a function of pump hydraulic efficiency and formulated in [12] for the first time under the conditions that there are no slip, preswirl-free and shock-free at BEPs in pump and turbine modes. Usually, for $\eta_{hp1} = \sqrt{\eta_{p1}}$ is kept [12], this group of conversion factors is expressed with pump total efficiency. Stepanoff proposed the following formulas for the three factors [12]

$$\begin{cases} q_1 = \eta_p^{-0.5} \\ h_1 = \eta_p^{-1} \\ \varepsilon_1 = 1 \end{cases} \tag{A3}$$

To improve prediction accuracy, assuming the pump and turbine mode share the same shaft power and total efficiency at BEPs and using existing specific speed relationship between pump and turbine, Sharma developed the three conversion

factors as follows [13]

$$\begin{cases} q_1 = \eta_{p1}^{-0.8} \\ h_1 = \eta_{p1}^{-1.2} \\ \varepsilon_1 = 1 \end{cases} \tag{A4}$$

Subsequently, Williams improved the formulas by multiplying a constant 1.1 on the term in the right-hand side in the first two factors in Eq. (A4) to account for the asymmetry of the efficiency curve in the turbine mode, namely [11]

$$\begin{cases} q_1 = 1.1\eta_{p1}^{-0.8} \\ h_1 = 1.1\eta_{p1}^{-1.2} \\ \varepsilon_1 = 1 \end{cases} \tag{A5}$$

At last, Alatorre-Frenk conducted curve fittings for a small set of data of pump and turbine modes, obtained the following formulas [11]

$$\begin{cases} q_1 = \dfrac{0.85\eta_{p1}^5 + 0.385}{2.0\eta_{p1}^{9.5} + 0.205} \\ h_1 = \dfrac{1}{0.85\eta_{p1}^5 + 0.385} \\ \varepsilon_1 = 1 \end{cases} \tag{A6}$$

Based on a simple theoretical consideration, a similar set of conversion factors was given in [14], and read as follows

$$\begin{cases} q_1 = 1.2\eta_{p1}^{-0.55} \\ h_1 = 1.2\eta_{p1}^{-1.1} \\ \varepsilon_1 = 1 \end{cases} \tag{A7}$$

The third group of conversion factors are based on specific speed only. Diederich provided two curves for flow rate and head conversion factors in terms of specific speed and presented approximately by the following expressions for a specific speed of 0.28–1.04 in [11]

$$\begin{cases} q_1 = 1.402K_p^{-0.171} \\ h_1 = 1.556K_p^{-0.174} \\ \varepsilon_1 = 1 \end{cases} \tag{A8}$$

This set of expressions is named as Diederich formula.

In [10], two plots of conversion factors were illustrated as a function specific speed and can be presented mathematically by the following equations in [11]

$$\begin{cases} q_1 = 1.86 - 0.551\ln(5K_p) + 0.11[\ln(5K_p)]^{2.2} \\ h_1 = 2.6 - 9.1\ln(5K_p) + 7.96[\ln(5K_p)]^{1.1} \\ \varepsilon_1 = 1 \end{cases} \tag{A9}$$

which are indicated as Gopalakrishnan formula.

The other kind of conversion factors is as a linear function of specific speed of pump was proposed by Grover in [11], when a specific speed is in a range of 0.2–1.1, the following empirical expression

$$\begin{cases} q_1 = 2.643 - 1.399K_p \\ h_1 = 2.693 - 1.212K_p \\ \varepsilon_1 = 0.893 + 0.0466K_p \end{cases} \tag{A10}$$

which are denoted by Grover formula.

Based on the experimental data of 11 end-suction centrifugal pumps as turbine, the following correlations are obtained to estimate the performance conversion factors at BEP in turbine mode in [15]

$$\begin{cases} h_1 = \left(0.0233\dfrac{n_p\sqrt{Q_{p1}}}{(gH_{p1})^{3/4}} + 0.6464\right)^{-2} \\ \dfrac{n_t\sqrt{Q_{t1}}}{(gH_{t1})^{3/4}} = 0.9413\dfrac{n_p\sqrt{Q_{p1}}}{(gH_{p1})^{3/4}} - 0.6045 \\ \dfrac{n_t\sqrt{\rho g Q_{t1}H_{t1}\eta_{t1}}}{\rho^{0.5}(gH_{t1})^{1.25}} = 0.849\dfrac{n_p\sqrt{\rho g Q_{p1}H_{p1}/\eta_{p1}}}{\rho^{0.5}(gH_{p1})^{1.25}} - 1.2376 \\ q_1 = \dfrac{Q_{t1}}{Q_{p1}}, h_1 = \dfrac{H_{t1}}{H_{p1}}, \varepsilon_1 = \dfrac{\eta_{t1}}{\eta_{p1}} \end{cases} \tag{A11}$$

where the same rotational speed is kept in both pump and turbine modes. The head conversion factor, h_1, is calculated from the first expression, and the flow rate, Q_{t1} can be estimated by means of the second one, then the turbine efficiency, η_{t1}, is figured out from the third expression. Finally, two conversion factors, q_1 and ε_1, can be work out accordingly.

In [16], an optimized performance conversion method was proposed to select a proper centrifugal pump for a specific turbine application based on 13 experimental data sets of pump as turbine. This method relies on two relationships, one is the empirical linear correlation of specific speed between pump and turbine modes at both BEPs, and the other is the empirical exponential function between Cordier turbine specific speed and specific diameter. If the geometrical and parameters of a pump are known at BEP, then the corresponding performance parameters in turbine model at BEP can be estimated by means of this method. Finally, the conversion factors can be figured out. Those relationships are written as [16]

$$\begin{cases} \dfrac{n_t\sqrt{Q_{t1}}}{H_{t1}^{3/4}} = 0.94\dfrac{n_p\sqrt{Q_{p1}}}{H_{p1}^{3/4}} - 3.12 \\ \dfrac{\left[\frac{4}{\pi^2}\frac{Q_{t1}}{(\frac{n_t}{60})d_{1t}^3}\right]^{1/2}}{\left[\frac{2}{\pi^2}\frac{gH_{t1}}{(\frac{n_t}{60})^2 d_{1t}^2}\right]^{3/4}} = \left\{\dfrac{\left[\frac{2}{\pi^2}\frac{gH_{t1}}{(\frac{n_t}{60})^2 d_{1t}^2}\right]^{1/4}}{\left[\frac{4}{\pi^2}\frac{Q_{t1}}{(\frac{n_t}{60})d_{1t}^3}\right]^{1/2}}\right\}^{-1.239} \\ q_1 = \dfrac{Q_{t1}}{Q_{p1}}, h_1 = \dfrac{H_{t1}}{H_{p1}}, \varepsilon_1 = 1 \end{cases} \tag{A12}$$

The forth group of conversion factors is in terms of both pump efficiency and specific speed. Initially, three conversion factors were proposed by Schmiedl [11], particularly, the flow rate and head conversion factors are just in terms of pump hydraulic efficiency, but the efficiency conversion factor is expressed as a function of specific speed alone, as follows for a specific speed in 0.1 and 1.05

$$\begin{cases} q_1 = -1.378 + 2.445/\eta_{hp1} \\ h_1 = -1.516 + 2.369/\eta_{hp1}^2 \\ \varepsilon_1 = 1.158 - 0.265K_p \end{cases} \tag{A13}$$

A series of experimental data of centrifugal pumps as turbine conducted by Chapallaz in literature were fitted in [11] in terms of specific speed and pump efficiency and the corresponding correlations are written as

$$\begin{cases} q_1 = 1.121\eta_{p1}^{-0.6}\left[1 + \left(0.4 + \ln K_{p1}\right)^2\right]^{0.15} \\ h_1 = 1.1\eta_{p1}^{-0.8}\left[1 + \left(0.3 + \ln K_{p1}\right)^2\right]^{0.3} \\ \varepsilon_1 = 1 - 0.03/\eta_{p1} \end{cases} \tag{A14}$$

here the expressions are entitled as Chapallaz formula.

In [11] the following flow rate, head and efficiency conversion factors for end-suction centrifugal pumps as turbines were proposed

$$\begin{cases} q_1 = 1.21\eta_{p1}^{-0.6} \\ h_1 = 1.21\eta_{p1}^{-0.8}\left[1+\left(0.6+\ln K_{p1}\right)^2\right]^{0.3} \\ \varepsilon_1 = 0.95\eta_{p1}^{-0.3}\left[1+\left(0.5+\ln K_{p1}\right)^2\right]^{-0.25} \end{cases} \tag{A15}$$

In [17], Nautiyal et al correlated the conversion factors at BEP to specific speed and total efficiency in pump mode based on their own experimental data and those found in relevant literature. Once again it was assumed the turbine efficiency is equal to the efficiency in the pump model at BEP. Those empirical expressions are presented as follows

$$\begin{cases} q_1 = 30.303\left(\eta_{p1}-0.212\right)/\ln\left(\dfrac{n_p\sqrt{Q_{p1}}}{H_{p1}^{3/4}}\right)-3.424 \\ h_1 = 41.667\left(\eta_{p1}-0.212\right)/\ln\left(\dfrac{n_p\sqrt{Q_{p1}}}{H_{p1}^{3/4}}\right)-5.042 \\ \varepsilon_1 = 1 \end{cases} \tag{A16}$$

References

[1] N. Koyama, Utilization of centrifugal pumps used as hydraulic turbines, J. Jpn. Soc. Mech. Eng. 74 (635) (1971) 1584–1587.
[2] B. Orchard, Pumps as turbines in water industry, World Pump 8 (2009) 22–23.
[3] H. Ramos, A. Borga, Pumps as turbines: an unconventional solution to energy production, Urban Water 1 (1999) 261–263.
[4] M. Arriaga, Pump as turbine–a pico-hydro alternative in Lao People's Democratic Republic, Renew. Energy 35 (2010) 1109–1115.
[5] T. Agarwal, Review of pump as turbine (PAT) for micro-hydropower, Int. J. Emerg. Technol. Adv. Eng. 2 (11) (2012) 163–169.
[6] H. Nautiyal, Varun, A. Kumar, Reverse running pumps analytical, experimental and computational study: a review, Renew. Sustain. Energy Rev. 14 (2010) 2059–2067.
[7] S.V. Jain, R.N. Patel, Investigations on pump running in turbine mode: a review of the state-of-the-art, Renew. Sustainable Energy Rev. 30 (2014) 841–868.
[8] R. Singh, S.V. Cabibbo, Hydraulic turbine energy recovery-R. O. system, Desalination 32 (1980) 281–296.
[9] W.A. Raja, R.W. Piazza, Reverse running centrifugal pumps as hydraulic power recovery turbines for seawater reverse osmosis systems, Desalination 38 (1980) 123–134.
[10] S. Gopalakrishnan, in: Proceedings of the 3rd International Pump User Symposium, Houston, USA, 1986.
[11] C. Alatorre-Frenk, Cost Minimisation in Micro-hydro Systems Using Pumps-as-Turbines, Ph.D Thesis, University of Warwick, UK, February 1994.
[12] A.J. Stepanoff, Centrifugal and Axial Flow Pumps, John Wiley, New York, 1957, pp. 270–271.
[13] A.A. Williams, The turbine performance of centrifugal pumps: a comparison of prediction methods, Proc. Instn. Mech. Eng., Part A: J. Power Energy 208 (1984) 59–66.
[14] S.S. Yang, S. Derakhshan, F.Y. Kong, Theoretical, numerical and experimental prediction of pump as turbine performance, Renew. Energy 48 (2012) 507–513.
[15] S. Derakhshan, A. Nourbakhsh, Theoretical, numerical and experimental investigation of centrifugal pumps in reverse operation, Exp. Therm. Fluid Sci. 32 (2008) 1620–1627.
[16] P. Singh, F. Nestmann, An optimization routine on a prediction and selection model for the turbine operation of centrifugal pumps, Exp. Therm. Fluid Sci. 34 (2010) 152–164.
[17] H. Nautiyal, Varun, A. Kumar, and S. Yadav, Experimental investigation of centrifugal pump working as turbine for small hydropower systems, Energy Sci. Technol. 1 1 (2011) 79–86.
[18] S. Derakhshan, A. Nourbakhsh, Experimental study of characteristic curves of centrifugal pumps working as turbines in different specific speeds, Exp. Therm. Fluid Sci. 32 (2008) 800–807.
[19] V.V. Jain, A. Swarnkar, K.H. Motwani, R.N. Patel, Effects of impeller diameter and rotational speed on performance of pump running in turbine mode, Energy Convers Manag 89 (2015) 808–824.
[20] J.C. Pascoa, F.J. Silva, J.S. Pinheiro, D.J. Martins, A new approach for predicting pat-pumping operating point from direct pumping mode characteristics, J. Sci. Ind. Res. 71 (2012) 144–148.
[21] N. Raman, I. Hussein, K. Palanisamy, B. Foo, An experimental investigation of pump as turbine for micro hydro application, in: Proceedings of IOP Conference Series Earth and Environmental Science, 16, 2013, pp. 1–4.
[22] H. Shinhama, J. Fukitomi, Y. Nakase, Y.T. Chen, T. Kuwauchi, S. Miyauchi, Study on reverse running pump turbine, Trans. Jpn. Soc. Mech. Eng. Ser. B 65 (638) (1999) 3399–3406.
[23] Y. Nakatake, Y. Kuma, A. Miyao, T. Kurokawa, Study on performance and improvement of efficiency for reverse running pump turbine, Mem. Kurume Nat. Coll. Technol. 17 (1) (2001) 1–6.
[24] J. Fernandez, E. Blanco, J. Parrondo, M.T. Stickland, T.J. Scanlon, Performance of a centrifugal pump running in inverse mode, Proc Instn Mech Engrs, Part A: J. Power Energy 218 (2004) 265–271.
[25] S. Rawal, J.T. Kshirsagar, Numerical simulation on a pump operating in a turbine mode, in: Proceedings of the 23rd International Pump User Symposium, Houston, USA, 2007.
[26] J. Gonzalez, J. Fernandez, K.M. Arguelles-Dıaz, C. Santolaria, Flow analysis for a double suction centrifugal machine in the pump and turbine operation modes, Int. J. Numer. Methods Fluids 61 (2009) 220–236.
[27] H. Nautiyal, V. Geol, A. Kumar, CFD analysis on pumps working as turbines, Hydro Nepal 6 (2010) 35–37.
[28] J.B. Bogdanovic-Jovanovic, D.R. Milenkovic, D.M. Svrkota, B. Bogdanovic, Z.T. Spasic, Pumps as turbines-power recovery, energy efficiency, CFD analysis, Therm. Sci. 18 (3) (2014) 1029–1040.
[29] C.S. Morros, J.M.F. Oro, K.M.A. Diaz, Numerical modelling and flow analysis of a centrifugal pump running as a turbine: unsteady flow structures and its effects on the global performance, Int. J. Numer. Methods Fluids 65 (2011) 542–562.
[30] R. Barrio, J. Fernandez, E. Blanco, J. Parrondo, A. Marcos, Performance characteristics and internal flow patterns in a reverse-running pump–turbine, Proc. Instn. Mech. Engrs. Part C: J. Mech. Eng. Sci. 226 (2011) 695–708.

[31] A. Couzinet, L. Gros, D. Pierrat, Characteristics of centrifugal pumps working in direct or reverse mode: focus on the unsteady radial thrust, Int. J. Rotat. Mach. 2013, 279049, 11pages.
[32] W.G. Li, Effects of viscosity on turbine mode performance and flow of a low specific speed centrifugal pump, Appl. Math. Model. 40 (2016) 904–926.
[33] W.G. Li, Mechanism for onset of sudden-rising head effect in centrifugal pump when handling viscous oils, ASME J. Fluids Eng. 136 (2014) 074501-1-10..
[34] W.G. Li, Effect of exit blade angle, viscosity and roughness in centrifugal pumps investigated by CFD computation, TASK Q. 15 (1) (2011) 21–41.
[35] Y.L. Zhang, Y. Li, Z.C. Zhu, B.L. Cui, Computational analysis of centrifugal pump delivering solid-liquid two-phase flow during startup period, Chin. J.Mech. Eng. 27 (1) (2014) 178–185.
[36] S.S. Yang, F.Y. Kong, W.M. Jiang, X.Y. Qu, Effects of impeller trimming influencing pump as turbine, Comput. Fluids 67 (2012) 72–78.